Table 1 Summary of characteristics of acute GBV-B infection in monkeys

Monkeys permissive of experimental infection	Tamarins (Genus *Saguinus*) Common marmoset (*Callithrix jacchus*) Owl monkey (*Aotus trivirgatus*)
Appearance of viremia	1–2 weeks post infection
Peak levels of viremia	Tamarins; 10^7–10^{10} GE/ml Marmoset and owl monkey; 10^5–10^8 GE/ml
Peak ALT levels	Approximately 200–500 IU/ml
Duration of viremia	2–3 months
Timing of seroconversion	A couple of weeks before clearance of viremia

persists for 2–3 months and is followed by clearance. GBV-B-infected monkeys with viremia usually develop self-resolving subacute hepatitis, as indicated by increases in the concentrations of serum enzymes such as ALT, gamma-glutamyltranspeptidase, and isocitrate dehydrogenase. Pathologically, degeneration and apoptosis of hepatocytes, as well as disruption and dilation of sinusoids, have been observed in the livers of GBV-B-infected tamarins with higher viremia and ALT activity (29). It is possible that GBV-B-specific CTL may cause the liver damage. However, a recent study reported that CTL are induced at a late stage of subacute GBV-B infection, and are inversely correlated with reduction in viremia (30). Since liver damage is usually found very early (1–2 weeks) after infection, when specific CTL are not observed, it is likely that viral replication in the hepatocytes leads directly to the early onset of cytopathic effects, while lower numbers of CTL may also contribute to cytotoxicity.

The clearance of viremia in the acute phase of GBV-B infection should require an effective antiviral immune response. In particular, in both GBV-B and HCV intrahepatic CTL appear to play a major role in viral clearance (30, 31). In addition, secondary GBV-B infection after clearance of the primary viremia induces a strong T cell response, leading to virtual absence of viremia, indicating that efficient memory is a key to protection from chronic viral infection (30, 32). In pre-immune chimpanzees antibody-mediated depletion of either CD4 or CD8 T lymphocytes affects their ability to control viral replication, resulting in prolonged viremia, demonstrating essential roles for both CD4 and CD8 memory in protection from viral persistence (33, 34).

On the other hand, the significance of humoral immunity in controlling GBV-B replication is still unclear. It is reasonable to assume that neutralizing antibodies also play important roles in the clearance of subacute viremia and protection from viral persistence. In the case of HCV, in one well characterized single-source outbreak of hepatitis C, viral clearance was associated with rapid induction of neutralizing antibodies in the early phase of infection, while chronic HCV infection was characterized by absent or low-titer neutralizing antibodies in this phase. Patients with resolution of infection were shown to exhibit broader cross-neutralizing activity of antibodies in the early phase of infection (35). In one chronic HCV patient who was followed up for 30 years, it has also been shown that HCV continuously escaped the host's immune system by repeated mutational changes, resulting in loss of recognition of the HCV envelope glycoproteins by antibodies (36). The fact that the sequences of envelope glycoprotein and specificity of neutralizing antibody change over time suggests that neutralizing antibodies exert selective pressure on HCV evolution. Thus, although neutralizing antibodies (and/or CTL) are not necessarily capable of controlling chronic viral infection, frequent escape from the antibodies needs so called fitness cost, resulting in the partial suppression of viral loads. Indeed, HCV-infected patients with primary antibody deficiencies have accelerated rates of disease progression (37).

Although features of the subacute phase of GBV-B infection are similar to that of HCV, a major defect of GBV-B infection as a surrogate model for HCV is that it is difficult to chronically infect monkeys. While as many as 70% of humans with HCV infection become chronically infected, only approximately a third of chimpanzees do so (2, 12). By contrast, only a few cases regarding chronic GBV-B infection have been reported so far. The best example was a case of a tamarin persistently infected with GBV-B (24); the monkey exhibited acute mild hepatitis with viremia (peak level; $\sim 10^9$ GE/ml), which reduced to a set point level (less than 10^4 GE/ml) at 16 weeks post infection, followed by a gradual increase in viremia which reached $>10^7$ GE/ml at 112 weeks post infection, along with a significant ALT increase. However, the viremia suddenly declined thereafter and became undetectable, in association with a reduction in antibody titer, and subsequent *in vivo* passage of virus obtained from the tamarin failed to reproduce persistent infection in other tamarins (24). In addition, immunosuppression of a GBV-B-infected tamarin by FK506 treatment, or infection of GBV-B with deletion of poly(U) tract in the 3′ UTR, reportedly resulted in relatively long-term persistent infection of GBV-B for up to 46 and 90 weeks, respectively (23, 27). These results indicate that GBV-B may have the potential for establishing chronic infection.

Furthermore, our recent study has demonstrated that among four common marmosets infected with GBV-B derived from a molecular clone pGBB (21), two developed long-term chronic infection for up to three years, with recurrent viremia in which plasma viral RNA levels fluctuated between undetectable and 10^5 GE/ml, which is equivalent to the case of chimpanzees chronically infected with

HCV (Iwasaki *et al.*, manuscript in preparation). Notably, the induction of antiviral antibody response as measured by anti-Core and -NS3 antibodies was delayed in both cases, followed by a gradual increase, and then sustained high antibody titers. This was in contrast with an abrupt and transient increase at the end of periods of subacute viremia in marmosets and tamarins with viral clearance. Whether a delayed antibody response is associated with persistent GBV-B infection remains to be determined.

Taken together, these findings indicate the similarity between HCV and GBV-B in regard to their ability to induce chronic infection, and also shed light on the further potential of GBV-B as a surrogate model for HCV.

FUTURE PROSPECT OF GBV-B SURROGATE MODEL

Although many questions are still to be addressed, accumulating evidence from extensive studies to date has greatly advanced the usefulness of the GBV-B as a surrogate model for HCV. The GBV-B model may be applicable for evaluating the feasibility and safety of anti-HCV vaccines employing novel viral vectors and gene therapy which creates RNA interference. For example, in a recent pilot study we showed that systemic administration of cationic liposome-encapsulated small interfering RNA to marmosets resulted in efficient regulation of GBV-B replication, indicating the usefulness of the surrogate model for proving the feasibility of RNA interference technology for future clinical application (38). This GBV-B model will also be helpful in identifying the virological and immunological factors which determine whether the outcome is acute resolving or chronic infection. While the GBV-B model appears to be valuable, development of an HCV/GBV-B chimeric virus would greatly expand the utility of the surrogate model, since it would enable us to directly evaluate antiviral vaccines and chemicals for HCV as a preclinical study. Rijnbrand *et al.* have reported that a chimeric GBV-B with 5′ untranslated region from HCV is infectious and causes hepatitis in tamarins (39). As recently demonstrated by Chevalier *et al.* (40), this will be a good model for evaluating the potential of small interfering RNA specific to HCV genome for future clinical application.

In regard to this, we may refer to an elegant precedent in the case of the macaques AIDS model. SIVmac is well known to efficiently infect, and result in the development of AIDS in macaques. Furthermore HIV-1, of which only 7% of the entire genome is derived from SIVmac, has been demonstrated to overcome the host range of authentic HIV-1, and to acquire the ability to productively infect macaque cells (41, 42). Instead of endangered chimpanzees, tamarins/marmosets which can be chronically infected with an HCV/GBV-B chimera (hopefully capable of inducing chronic hepatitis) should be the next generation of a promising non-human primate surrogate model for HCV infection, one which is similar to the macaques AIDS model. Whatever animals are used for pre-clinical study, it is important to keep in mind that results obtained from monkey models using either GBV-B or HCV/GBV-B chimera (as well as SIV or HIV/SIV chimera) may not necessarily be applicable to humans, because of potential differences in the molecular structure and/or mechanism by which antivirals and/or viral and host proteins function. Further characterization and understanding of the molecular biology and immunology of virus-host interactions will help in developing novel antiviral strategies.

REFERENCES

1. Choo Q.L., Kuo G., Weiner A.J., Overby L.R., Bradley D.W., Houghton M. (1989) Isolation of a cDNA clone derived from a blood-borne non-A, non-B viral hepatitis genome. *Science* **244:** 359–62.
2. Chisari F.V. (2005) Unscrambling hepatitis C virus-host interactions. *Nature* **436:** 930–32.
3. Alter M.J. (2007) Epidemiology of hepatitis C virus infection. *World J Gastroenterol* **13:** 2436–441.
4. Feld J.J., Hoofnagle J.H. (2005) Mechanism of action of interferon and ribavirin in treatment of hepatitis C. *Nature* **436:** 967–72.
5. Kremsdorf D., Brezillon N. (2007) New animal models for hepatitis C viral infection and pathogenesis studies. *World J Gastroenterol* **13:** 2427–435.
6. Wu G.Y., Konishi M., Walton C.M., Olive D., Hayashi K., Wu C.H. (2005) A novel immunocompetent rat model of HCV infection and hepatitis. *Gastroenterology* **128:** 1416–423.
7. Ilan E., Arazi J., Nussbaum O., Nussbaum O., Zauberman A., Eren R., Lubin I., Neville L., Ben-Moshe O., Kischitzky A., Litchi A., Margalit I., Gopher J., Mounir S., Cai W., Daudi N., Eid A., Jurim O., Czerniak A., Galun E., Dagan S. (2002) The hepatitis C virus (HCV)-Trimera mouse: a model for evaluation of agents against HCV. *J Infect Dis* **185:** 153–61.
8. Eren R., Landstein D., Terkieltaub D., Nussbaum O., Zauberman A., Ben-Porath J., Gopher J., Buchnick R., Kovjazin R., Rosenthal-Galili Z., Aviel S., Ilan E., Shoshany Y., Neville L., Waisman T., Ben-Moshe O., Kischitsky A., Foung S.K., Keck Z.Y., Pappo O., Eid A., Jurim O., Zamir G., Galun E., Dagan S. (2006) Preclinical evaluation of two neutralizing human monoclonal antibodies against hepatitis C virus (HCV): a potential treatment to prevent HCV reinfection in liver transplant patients. *J Virol* **80:** 2654–664.
9. Mercer D.F., Schiller D.E., Elliott J.F., Douglas D.N., Hao C., Rinfret A., Addison W.R., Fischer K.P., Churchill T.A., Lakey J.R., Tyrrell D.L., Kneteman N.M. (2001) Hepatitis C virus replication in mice with chimeric human livers. *Nat Med* **7:** 927–33.
10. Meuleman P., Libbrecht L., De Vos R., de Hemptinne B., Gevaert K., Vandekerckhove J., Roskams T., Leroux-Roels G. (2005) Morphological and biochemical characterization of a human liver in a uPA-SCID mouse chimera. *Hepatology* **41:** 847–56.
11. Kneteman N.M., Weiner A.J., O'Connell J., Collett M., Gao T., Aukerman L., Kovelsky R., Ni Z.J., Zhu Q., Hashash A., Kline J., Hsi B., Schiller D., Douglas D., Tyrrell D.L., Mercer D.F. (2006) Anti-HCV therapies in chimeric scid-Alb/uPA mice parallel outcomes in human clinical application. *Hepatology* **43:** 1346–353.

12. Bassett S.E., Brasky K.M., Lanford R.E. (1998) Analysis of hepatitis C virus-inoculated chimpanzees reveals unexpected clinical profiles. *J Virol* **72:** 2589–599.
13. Cohen J. (2007) Animal studies: NIH to end chimp breeding for research. *Science* **316:** 1265.
14. Ambrose Z., KewalRamani V.N., Bieniasz P.D., Hatziioannou T. (2007) HIV/AIDS: in search of an animal model. *Trends Biotech* **25:** 333–37.
15. Lackner A.A., Veazey R.S. (2007) Current concepts in AIDS pathogenesis: insights from the SIV/macaque model. *Annu Rev Med* **58:** 461–76.
16. Deinhardt F., Holmes A.W., Capps R.B., Popper H. (1967) Studies on the transmission of human viral hepatitis to marmoset monkeys. I. Transmission of disease, serial passages, and description of liver lesions. *J Exp Med* **125:** 673–88.
17. Simons J.N., Pilot-Matias T.J., Leary T.P., Dawson G.J., Desai S.M., Schlauder G.G., Muerhoff A.S., Erker J.C., Buijk S.L., Chalmers M.L. (1995) Identification of two flavivirus-like genomes in the GB hepatitis agent. *Proc Natl Acad Sci USA* **92:** 3401–405.
18. Schaluder G.G., Dawson G.J., Simons J.N., Pilot-Matias T.J., Gutierrez R.A., Heynen C.A., Knigge M.F., Kurpiewski G.S., Buijk S.L., Leary T.P., Muerhoff A.S., Desai S.M., Mushahwar I.K. (1995) Molecular and serologic analysis in the transmission of the GB hepatitis agents. *J Med Virol* **46:** 81–90.
19. Bukh J., Apgar C.L., Govindarajan S., Purcell R.H. (2001) Host range studies of GB virus-B hepatitis agent, the closest relative of hepatitis C virus, in New World monkeys and chimpanzees. *J Med Virol* **65:** 694–97.
20. Beames B., Chavez D., Lanford R.E. (2001) GB virus B as a model for hepatitis C virus. *ILAR J* **42:** 152–60.
21. Bukh J., Apgar C.L., Yanagi M. (1999) Toward a surrogate model for hepatitis C virus: An infectious molecular clone of the GB virus-B hepatitis agent. *Virology* **262:** 470–78.
22. Sbardellati A., Scarselli E., Verschoor E., De Tomassi A., Lazzaro D., Traboni C. (2001) Generation of infectious and transmissible virions from a GB virus B full-length consensus clone in tamarins. *J Gen Virol* **82:** 2437–448.
23. Lanford R.E., Chavez D., Notvall L., Brasky K.M. (2003) Comparison of tamarins and marmosets as hosts for GBV-B infections and the effect of immunosuppression on duration of viremia. *Virology* **311:** 72–80.
24. Martin A., Bodola F., Sangar D.V., Goettge K., Popov V., Rijnbrand R., Lanford R.E., Lemon S.M. (2003) Chronic hepatitis associated with GB virus B persistence in a tamarin after intrahepatic inoculation of synthetic viral RNA. *Proc Natl Acad Sci USA* **100:** 9962–967.
25. Bright H., Carroll A.R., Watts P.A., Fenton R.J. (2004) Development of a GB virus B marmoset model and its validation with a novel series of hepatitis C virus NS3 protease inhibitors. *J Virol* **78:** 2062–071.
26. Jacob J.R., Lin K.C., Tennant B.C., Mansfield K.G. (2004) GB virus B infection of the common marmoset (*Callithrix jacchus*) and associated liver pathology. *J Gen Virol* **85:** 2525–533.
27. Nam J.H., Faulk K., Engle R.E., Govindarajan S., St Claire M., Bukh J. (2004) *In vivo* analysis of the 3′ untranslated region of GB virus B after *in vitro* mutagenesis of an infectious cDNA clone: persistent infection in a transfected tamarin. *J Virol* **78:** 9389–399.
28. Kyuregyan K.K., Poleschuk V.F., Zamyatina N.A., Isaeva O.V., Michailov M.I., Ross S., Bukh J., Roggendorf M., Viazov S. (2005) Acute GB virus B infection of marmosets is accompanied by mutations in the NS5A protein. *Virus Res* **114:** 154–57.
29. Ishii K., Iijima S., Kimura N., Lee Y.J., Ageyama N., Yagi S., Yamaguchi K., Maki N., Mori K., Yoshizaki S., Machida S., Suzuki T., Iwata N., Sata T., Terao K., Miyamura T., Akari H. (2007) GBV-B as a pleiotropic virus: distribution of GBV-B in extrahepatic tissues *in vivo*. *Microbes Infect* **9:** 515–21.
30. Woollard D.J., Haqshenas G., Dong X., Pratt B.F., Kent S.J., Gowans E.J. (2008) Virus-specific T-cell immunity correlates with control of GBV-B infection in marmosets. *J Virol* **82:** 3054–060.
31. Neumann-Haefelin C., Spangenberg H.C., Blum H.E., Thimme R. (2007) Host and viral factors contributing to CD8+ T cell failure in hepatitis C virus infection. *World J Gastroenterol* **13:** 4839–847.
32. Bukh J., Engle R.E., Govindarajan S., Purcell R.H. (2008) Immunity against the GBV-B hepatitis virus in tamarins can prevent productive infection following rechallenge and is long-lived. *J Med Virol* **80:** 87–94.
33. Shoukry N.H., Grakoui A., Houghton M., Chien D.Y., Ghrayeb J., Reimann K.A., Walker C.M. (2003) Memory CD8+ T cells are required for protection from persistent hepatitis C virus infection. *J Exp Med* **197:** 1645–655.
34. Grakoui A., Shoukry N.H., Woollard D.J., Han J.H., Hanson H.L., Ghrayeb J., Murthy K.K., Rice C.M., Walker C.M. (2003) HCV persistence and immune evasion in the absence of memory T cell help. *Science* **302:** 659–62.
35. Pestka J.M., Zeisel M.B., Bläser E., Schürmann P., Bartosch B., Cosset F.L., Patel A.H., Meisel H., Baumert J., Viazov S., Rispeter K., Blum H.E., Roggendorf M., Baumert T.F. (2007) Rapid induction of virus-neutralizing antibodies and viral clearance in a single-source outbreak of hepatitis C. *Proc Natl Acad Sci USA* **104:** 6025–030.
36. von Hahn T., Yoon J.C., Alter H., Rice C.M., Rehermann B., Balfe P., McKeating J.A. (2007) Hepatitis C virus continuously escapes from neutralizing antibody and T-cell responses during chronic infection *in vivo*. *Gastroenterology* **132:** 667–78.
37. Chapel H.M., Christie J.M., Peach V., Chapman R.W. (2001) Five-year follow-up of patients with primary antibody deficiencies following an outbreak of acute hepatitis C. *Clin Immunol* **99:** 320–24.
38. Yokota T., Iijima S., Kubodera T., Ishii K., Katakai Y., Ageyama N., Chen Y., Lee Y.J., Unno T., Nishina K., Iwasaki Y., Maki N., Mizusawa H., Akari H. (2007) Efficient regulation of viral replication by siRNA in a non-human primate surrogate model for hepatitis C. *Biochem Biophys Res Commun* **361:** 294–300.
39. Rijnbrand R., Yang Y., Beales L., Bodola F., Goettge K., Cohen L., Lanford R.E., Lemon S.M., Martin A. (2005) A chimeric GB virus B with 5′ nontranslated RNA sequence from hepatitis C virus causes hepatitis in tamarins. *Hepatology* **41:** 986–94.
40. Chevalier C., Saulnier A., Benureau Y., Fléchet D., Delgrange D., Colbère-Garapin F., Wychowski C., Martin A. (2007) Inhibition of hepatitis C virus infection in cell culture by small interfering RNAs. *Mol Ther* **15:** 1452–462.
41. Kamada K., Igarashi T., Martin M.A., Khamsri B., Hatcho K., Yamashita T., Fujita M., Uchiyama T., Adachi A. (2006) Generation of HIV-1 derivatives that productively infect macaque monkey lymphoid cells. *Proc Natl Acad Sci USA* **103:** 16959–6964.
42. Hatziioannou T., Princiotta M., Piatak M. Jr, Yuan F., Zhang F., Lifson J.D., Bieniasz P.D. (2006) Generation of simian-tropic HIV-1 by restriction factor evasion. *Science* **314:** 95.

THE JOURNAL OF BIOLOGICAL CHEMISTRY VOL. 284, NO. 2, pp. 807–817, January 9, 2009

Riplet/RNF135, a RING Finger Protein, Ubiquitinates RIG-I to Promote Interferon-β Induction during the Early Phase of Viral Infection*[S]

Received for publication, June 3, 2008, and in revised form, November 10, 2008 Published, JBC Papers in Press, November 18, 2008, DOI 10.1074/jbc.M804259200

Hiroyuki Oshiumi[‡], Misako Matsumoto[‡], Shigetsugu Hatakeyama[§], and Tsukasa Seya[‡1]

From the [‡]Department of Microbiology and Immunology and the [§]Department of Biochemistry, Hokkaido University Graduate School of Medicine, Kita-15, Nishi-7, Kita-ku Sapporo 060-8638, Japan

RIG-I (retinoic acid-inducible gene-I), a cytoplasmic RNA helicase, interacts with IPS-1/MAVS/Cardif/VISA, a protein on the outer membrane of mitochondria, to signal the presence of virus-derived RNA and induce type I interferon production. Activation of RIG-I requires the ubiquitin ligase, TRIM25, which mediates lysine 63-linked polyubiquitination of the RIG-I N-terminal CARD-like region. However, how this modification proceeds for activation of IPS-1 by RIG-I remains unclear. Here we identify an alternative factor, Riplet/RNF135, that promotes RIG-I activation independent of TRIM25. The Riplet/RNF135 protein consists of an N-terminal RING finger domain, C-terminal SPRY and PRY motifs, and shows sequence similarity to TRIM25. Immunoprecipitation analyses demonstrated that the C-terminal helicase and repressor domains of RIG-I interact with the Riplet/RNF135 C-terminal region, whereas the CARD-like region of RIG-I is dispensable for this interaction. Riplet/RNF135 promotes lysine 63-linked polyubiquitination of the C-terminal region of RIG-I, modification of which differs from the N-terminal ubiquitination by TRIM25. Overexpression and knockdown analyses revealed that Riplet/RNF135 promotes RIG-I-mediated interferon-β promoter activation and inhibits propagation of the negative-strand RNA virus, vesicular stomatitis virus. Our data suggest that Riplet/RNF135 is a novel factor of the RIG-I pathway that is involved in the evoking of human innate immunity against RNA virus infection, and activates RIG-I through ubiquitination of its C-terminal region. We infer that a variety of RIG-I-ubiquitinating molecular complexes sustain RIG-I activation to modulate RNA virus replication in the cytoplasm.

Cytoplasmic viral RNA sensors induce production of type I interferon (IFN)[2] (1, 2). Representative cytoplasmic sensors, RIG-I-like receptors (RLRs) of RIG-I, MDA5, and LGP2, belong to the DEA(D/H) box RNA helicase family (3–6). RIG-I recognizes the 5′ end triphosphate of the virus RNA genome or double-stranded RNA (6–8) to sense infection by various RNA viruses (3, 5). The RIG-I protein consists of two N-terminal CARD-like domains, an RNA helicase region and a repressor domain (RD) (9). After recognition of positive or negative single-stranded viral RNA, RIG-I interacts with its adaptor molecule IPS-1/MAVS/Cardif/VISA leading to type I IFN production, thereby protecting host cells from amplified viral replication (10–13). However, only a few copies of viral RNAs usually penetrate the cell membrane to enter the cell at an early infection, and these RLRs are barely present in intact as well as early virus-infected cells (6). The early viral RNA recognition facility should be different from that of the late phase when RIG-I protein is abundant in the cytoplasm and easily re-organizes the virus RNAs. What molecular mechanism is responsible for initial sensing of viral RNA thus remains unknown.

Other RLRs, MDA5 and LGP2, are structurally similar to RIG-I in their having the helicase domain (5, 14). However, MDA5 lacks the RD domain although it possesses CARD-like region at the N terminus like RIG-I. LGP2 does not have a CARD-like region but possesses RD at its C terminus (9). RIG-I and MDA5 recognize different kinds of RNA viruses and in some cases play a redundant role in sensing virus infection, such as influenza B (15). In contrast, LGP2 rather negatively regulates virus replication. LGP2 expression suppressed RIG-I or MDA5 signaling (14, 16), and *lgp2* gene disruption conferred high susceptibility to virus infection on mice (4).

Recently, the majority of proteins involved in the type I IFN-inducing system were found ubiquitinated. For example, the tumor necrosis factor receptor-associated family members, TRAF3 and TRAF6, are ubiquitin ligases to induce ubiquitination of proteins and implicated in activation of IFN regulatory factor (IRF) 3 or nuclear factor (NF) κB (13, 17–19). In contrast, a deubiquitinating enzyme, DUBA or A20, suppresses these signals (19, 20). In addition to ubiquitin, ubiquitin-like protein, ISG15, is also conjugated to proteins involved in the IFN-inducing pathway (21, 22). Recent studies have revealed that viral RNA sensors are also ubiquitinated. TRIM25 (ZNF147 or EFP), a member of the ubiquitin-protein isopeptide ligase family, which possesses a RING finger domain, ubiquitinates the

* This work was supported in part by grants-in-aid from the Ministry of Education, Science and Culture of Japan, Ministry of Health, Labour, and Welfare, The Mitsubishi Foundation, and The Mochida Memorial Foundation. The costs of publication of this article were defrayed in part by the payment of page charges. This article must therefore be hereby marked "*advertisement*" in accordance with 18 U.S.C. Section 1734 solely to indicate this fact.

[S] The on-line version of this article (available at http://www.jbc.org) contains supplemental Figs. S1–S6.

The nucleotide sequence(s) reported in this paper has been submitted to the GenBank™/EBI Data Bank with accession number(s) AB470605.

[1] To whom correspondence should be addressed: Dept. of Microbiology and Immunology, Graduate School of Medicine, Hokkaido University, Kita-ku, Sapporo 060-8638, Japan. Tel.: 81-11-706-5073; Fax: 81-11-706-7866; E-mail: seya-tu@pop.med.hokudai.ac.jp.

[2] The abbreviations used are: IFN, interferon; RT, reverse transcription; RLR, RIG-I-like receptor; HA, hemagglutinin; siRNA, small interference; m.o.i., multiplicity of infection; VSV, vesicular stomatitis virus; IRF, IFN regulatory factor; Ub, ubiquitin; ORF, open reading frame; RD, repressor domain.

CARD-like domains of RIG-I thereby facilitating the RIG-I-mediated activation of type I IFN signaling (23, 24), although Shimotohno and co-workers (25) previously reported that TRIM25 (EFP) does not polyubiquitinate the RIG-I CARD-like region as far under their conditions. Expression of TRIM25 increases RIG-I CARD-like region-mediated signaling; however, it remains to be determined whether the activation of full-length RIG-I requires other ubiquitin ligase (23). Another ubiquitin ligase RNF125 mediates lysine 48-linked polyubiquitination of RIG-I, which leads to degradation of RIG-I through the proteasome (25).

Here we examined what molecular complex participates in an early RIG-I-mediated RNA recognition and IFN signaling by yeast two-hybrid screening. Here we detected two novel RING finger proteins that bound to RIG-I, and we found that one, RNF135, facilitated RIG-I-mediated type I IFN induction via ubiquitinating RIG-I. RNF135 plays a crucial role in the RIG-I response to minimal copies of viral RNA, and by binding to the C-terminal helicase and RD regions of RIG-I, RNF135 facilitates RIG-I C-terminal ubiquitination to up-regulate RIG-I-mediated IFN signaling and suppress viral replication. Hence, we renamed it as RNF135 Riplet (RING finger protein leading to RIG-I activation). To our knowledge, this is the first study demonstrating that C-terminal ubiquitination of RIG-I is important for full IFN induction by RIG-I.

EXPERIMENTAL PROCEDURES

Cell Cultures—HEK293 and Vero cells were cultured in Dulbecco's modified Eagle's medium with 10% fetal calf serum (Invitrogen), and HeLa cells were in minimum Eagle's medium with 2 mM L-glutamine and 10% fetal calf serum (JRH Biosciences). HEK293FT cells were maintained in Dulbecco's modified Eagle's high glucose medium containing 10% heat-inactivated fetal calf serum (Invitrogen).

Plasmids—cDNA fragment encoding a C-terminal region of Riplet was isolated by yeast two-hybrid screening using human lung cDNA library. The 5′ region encoding the remaining N-terminal region was amplified by PCR using primers Riplet-F1 and Riplet-R1, and human lung cDNA library was used for its template. Two cDNA fragments, which cover the entire ORF of Riplet, were joined by PCR using primers Riplet-F1, R1, F2, and R2 and then inserted into pCR-blunt vector (Invitrogen). The primers sequences are as follows: F1, GCCTCGAGGCCACCATGGCGGGCCTGGGCCTGGG; R1, CGGCCAGGTCCTGCAGTAGC; F2, GCACCTGCGGAAGAACACGC; and R2, GGGGATCCCACCTTTACTTGCTTTATTATCAGG. The obtained cDNA was cloned into XhoI-NotI restriction sites of pEF-BOS expression vector, and the HA tag was fused at the C-terminal end of Riplet. Riplet-DN (dominant negative) expression vector was constructed by amplifying the relevant Riplet cDNA fragment using the primers Riplet-X-F-C and Riplet-R2 and subcloned into pEF-BOS. The primer sequence of Riplet-X-F-C was as follows: GCTCGAGGCCACCATGCCGCACCTGCGGAAGAACACGC. Riplet-L248fs expression vector was made by deleting 1 base at position 742 by standard PCR-mediated site-directed mutagenesis methods with primers Riplet-L248fs-F and Riplet-L248fs-R as follows: Riplet-L248fs-F, CCAGAGCCACCCTGCATCAGGAGAGCTTCTCGG, and Riplet-L248fs-R, CCGAGAAGCTCTCCTGATGCAGGGTGGCTCTGG. All cloned *RIPLET* cDNA fragments were sequenced, and it was confirmed that there were no mutations. Full-length RIG-I expressing vector, Gal4-IRF-3, Gal4-DBD, and p55 UASG-Luc reporter plasmids were gifts from Dr. T. Fujita (Kyoto University, Kyoto, Japan). p125 luc reporter plasmid was a gift from Dr. T. Taniguchi (University of Tokyo, Tokyo, Japan). RIG-I RD expressing vector was made with primers RIG-I RD-F and RIG-I RD-R; the RIG-I dRD cDNA fragment, which encodes ORF of RIG-I from the 1- to 754-amino acid region, was made by using primers RIG-I-(1–754)F and RIG-I-(1–754)R. The obtained cDNA fragments were sequenced, and it was confirmed that there were no mutations caused by PCR. The primers sequences are as follows: RIG-I RD-F, GAT GAT AAA GGT ACC ACC GGT AGC AAG TGC TTC CTT CTG; RIG-I RD-R, AAG GAA GCA CTT GCT ACC GGT GGT ACC TTT ATC ATC ATC ATC; RIG-I-(1–754)F, GC AGA GGA AGA GCA AGA TGA TAT CAG GTC CTC AAT CTT C; and RIG-I-(1–754)R, ATT GAG GAC CTG ATA TCA TCT TGC TCT TCC TCT GCC TC.

Northern Blotting—Human *RIPLET* 1092-bp cDNA fragment (208–1299) was used for the probe for Northern blotting. The Northern blot membranes, human 12-lane MTN blot and MTN blot III, were purchased from Clontech. The homology of human *RIPLET* and *TRIM25* in the probe region was 46%. We used a stringent condition for Northern blotting to exclude the cross-hybridization between the *RIPLET* and *TRIM25* genes. Briefly, the probe was labeled with [α-^{32}P]dCTP using Rediprime II Random Prime labeling system (GE Healthcare). The labeled probe was hybridized to the membrane with ExpressHyb hybridization solution (Clontech) at 68 °C for 1 h. The membrane was washed with washing solution I (2× SSC, 0.05% SDS) for 40 min, and then washed with washing solution II (0.1× SSC, 0.1% SDS) for 40 min. Riplet mRNA bands were detected with x-ray film.

Reporter Gene Analysis—HEK293 cells were transiently transfected in 24-well plates using FuGENE HD (Roche Applied Science) with expression vectors, reporter plasmids, and internal control plasmid coding *Renilla* luciferase. The total amounts of plasmids were normalized with empty vector. For poly(I-C) stimulation, 24 h after transfection, cells were stimulated with medium containing poly(I-C) (50 μg/ml) and DEAE-dextran (0.5 mg/ml) for 1 h, and then the medium was exchanged with normal medium and incubated for an additional 3 h. Cells were lysed with lysis buffer (Promega) and luciferase, and *Renilla* luciferase activities were measured by the dual luciferase assay kit (Promega). Relative luciferase activities were calculated by normalizing luciferase activity by *Renilla* luciferase activity, and dividing the normalized value by control in which only empty vector, reporter, and internal control plasmid were transfected. Values are expressed as mean relative stimulations ± S.D. for a representative experiment, and each was performed three times in duplicate (unless otherwise indicated in the legends).

RNA Interference—Reporter and siRNA (20 nM final concentration) for Riplet or control were transfected into HEK293 cells with Lipofectamine 2000 (Invitrogen) by the standard method described in the manufacturer's protocol. Empty vec-

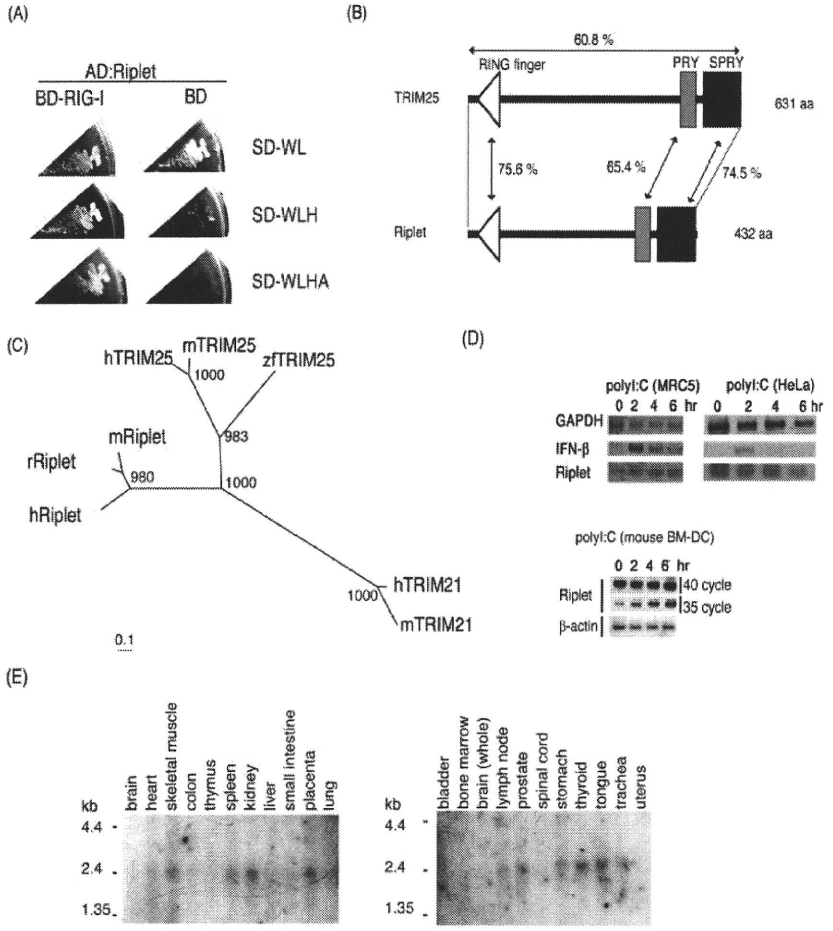

FIGURE 1. **Isolation of Riplet by yeast two-hybrid screening.** *A*, yeast cells carrying both RIG-I and Riplet can grow in selective media (SD-WLH, SD-WLHA), whereas yeast cells carrying RIG-I alone only grow in nonselective media (SD-WL), indicating the physical interaction of RIG-I with Riplet. *B*, human Riplet protein sequence is 60.8% identical to human TRIM25. The RING finger domains and SPRY motifs show higher sequence similarities between the two proteins. *aa*, amino acids. *C*, phylogenetic tree constructed by the Neighbor-Joining method shows that Riplet is similar to TRIM25. *h*, *m*, *r*, or *zf* represent human, mouse, rat, or zebrafish, respectively. The *numbers* on the node are bootstrap probabilities (n = 1000). *D*, HeLa cell, human primary-cultured fibroblast cell, MRC5, or bone marrow-derived mouse dendritic cell (*BM-DC*) were stimulated with poly(I-C) (50 μg/ml) for indicated hours. Total RNA was extracted with TRIzol reagent, and then RT-PCR was carried out using primers shown under "Experimental Procedures." *GAPDH*, glyceraldehyde-3-phosphate dehydrogenase. *E*, Northern blot membranes containing 1 μg of poly(A)$^+$ RNA per lane from human tissues were blotted with human Riplet probe.

tor was added to normalize the final plasmid amount. 48 h after transfection, cells were stimulated with poly(I-C) for 4 h. For VSV infection, 24 h after transfection, cells were infected with VSV at m.o.i. = 1, and cell lysate was prepared after 12 h for reporter gene assays. The degree of gene silencing was confirmed by RT-PCR using RNA extracted from cells 24 h after transfection. PCR primers used for the RT-PCR were Riplet-F3 (ACTGGGAAGTGGACACTAGG) and Riplet-R3 (ACTCATACAGAAGCTTCTCC). siRNAs were purchased from Funakoshi Co., Ltd. (Tokyo Japan), and the siRNA sequences of Riplet siRNA were GACUAUGGACUCUUGUUGUGU (sense) and ACAACAAGAGUCCAUAGUCCU (antisense). Control siRNA sequences were CUGUUGGUUUAGUAAGCCUGU (sense) and AGGCUUACUAAACCAACAGUC (antisense). Another siRNA, Riplet si-1, and control negative siRNA (silencer negative control 1 siRNA, AM4611) were purchased from Applied Biosystems. siRNA sequences were Riplet si-1 GGGAAAGCUUGCCUUCUAUdTdT (sense) and AUAGAAGGCAAGCUUUCCCdTdC (antisense).

Virus Preparation and Infection—VSV Indiana strain and poliovirus were amplified using Vero cells. HEK293 cells were transfected in 24-well plates with plasmid encoding *RIG-I*, Riplet, or no insert. 24 h after transfection, cells were infected with viruses for 24 h, and the titers of virus in culture supernatant were measured by plaque assay using Vero cells. For RNA interference assay, cells were transfected with siRNA with Lipofectamine 2000. 24 h after transfection, cells were infected with viruses at m.o.i. = 0.001 for 18 h, and the titer in culture supernatant were determined by plaque assay.

Immunoprecipitation—HEK293FT cells were transfected in 6-well plates with plasmids encoding FLAG-tagged RIG-I and/or HA-tagged Riplet. The plasmid amounts were normalized by the addition of empty plasmid. 24 h after transfection, cells were lysed with lysis buffer (20 mM Tris-HCl (pH 7.5), 125 mM NaCl, 1 mM EDTA, 10% glycerol, 1% Nonidet P-40, 30 mM NaF, 5 mM Na_3VO_4, 20 mM iodoacetamide, and 2 mM phenylmethylsulfonyl fluoride), and then proteins were immunoprecipitated with rabbit anti-HA polyclonal (Sigma) or anti-FLAG M2 monoclonal antibody (Sigma). The precipitated samples were analyzed by SDS-PAGE and stained with anti-HA (HA1.1) (Covance) or anti-FLAG M2 monoclonal antibody. For ubiquitination assay of RIG-I, the plasmid encoding two multiple HA-tagged ubiquitins was used. HEK293FT cells were transfected with plasmids encoding FLAG-tagged RIG-I, Riplet, or 2× HA-tagged ubiquitin. 24 h after transfection, cells were lysed, and then RIG-I was immunoprecipitated as described above. The samples were analyzed by SDS-PAGE and stained with anti-HA polyclonal antibody (for detection of ubiquitination) or anti-FLAG monoclonal antibody (for detection of RIG-I). Reproducibility was confirmed with additional experiments (see supplemental figures).

Construction of RIG-I 3KA and 5KA Mutant Genes—The C-terminal three or five lysine residues were mutated into alanines (designated as 3KA and 5KA). RIG-I 3KA has K888A, K907A, and K909A, whereas RIG-I 5KA has K849A, K851A,

K888A, K907A, and K909A. The mutant *rig-I* genes were made by PCR-mediated site-directed mutagenesis. The primers used for the PCR were as follows: K907–909A-forward, GTT CAG ACA CTG TAC TCG GCG TGG GCG GAC TTT CAT TTT GAG AAG, and K907–909A-reverse, CTT CTC AAA ATG AAA GTC CGC CCA CGC CGA GTA CAG TGT CTG AAC; K888A-forward, GAC ATT TGA GAT TCC AGT TAT AGC AAT TGA AAG TTT TGT GGT GGA GG, and K888A-reverse, CCT CCA CCA CAA AAC TTT CAA TTG CTA TAA CTG GAA TCT CAA ATG TC; K849–851A-forward, GAG TAG ACC ACA TCC CGC CCA GCG CAG TTT TCA AGT TTT G, and K849–851A-reverse, CAA AAC TTG AAA ACT GCG CTG GCG CGG GAT GTG GTC TAC TC. PCR was carried with Pyrobest *Taq* polymerase, and the obtained clones were sequenced to exclude the clones harboring PCR error. To construct the plasmid-expressing mutant RIG-I protein, the wild-type *RIG-I* gene on pEF-BOS vector was replaced with the mutant *rig-I* gene.

Real Time PCR—Quantitative PCR analyses were carried out using iCycler iQ real time detection system with Platinum SYBR Green qPCR SuperMix-UDG reagent (Invitrogen). Primer sequences for qPCR were as follows: hGAPDH-qF, GAG TCA ACG GAT TTG GTC GT, and hGAPDH-qR, TTG ATT TTG GAG GGA TCT CG; hIFN-β-qF, TGG GAG GAT TCT GCA TTA CC, and hIFN-β-qR, CAG CAT CTG CTG GTT GAA GA; hMx1-qF, ACC ACA GAG GCT CTC AGC AT, and hMx1-qR, CTC AGC TGG TCC TGG ATC TC; and hIFIT-1-qF, GCA GCC AAG TTT TAC CGA AG, and hIFIT-1-qR, CAC CTC AAA TGT GGG CTT TT. Values were expressed as mean relative stimulations, and for a representative experiment from a minimum of three separate experiments, each was performed in triplicate.

RESULTS

RIG-I-binding Proteins—To isolate the proteins that bind to RIG-I, we performed yeast two-hybrid screening using a human lung cDNA library. Using the RIG-I central region (213–601 amino acids), we isolated a clone that encoded a partial ORF of a gene expressed in a dendritic cell line, DC12, whereas the C-terminal region of RIG-I (557–925 amino acids) resulted in the isolation of two cDNA clones, which encoded partial C-terminal regions of ZNF598 and RNF135 (Fig. 1*A* and data not shown). Preliminary expression studies showed that the RNF135 segment affected the RIG-I IFN-β inducing activity, whereas the other two proteins had no effect (data not shown). We confirmed the

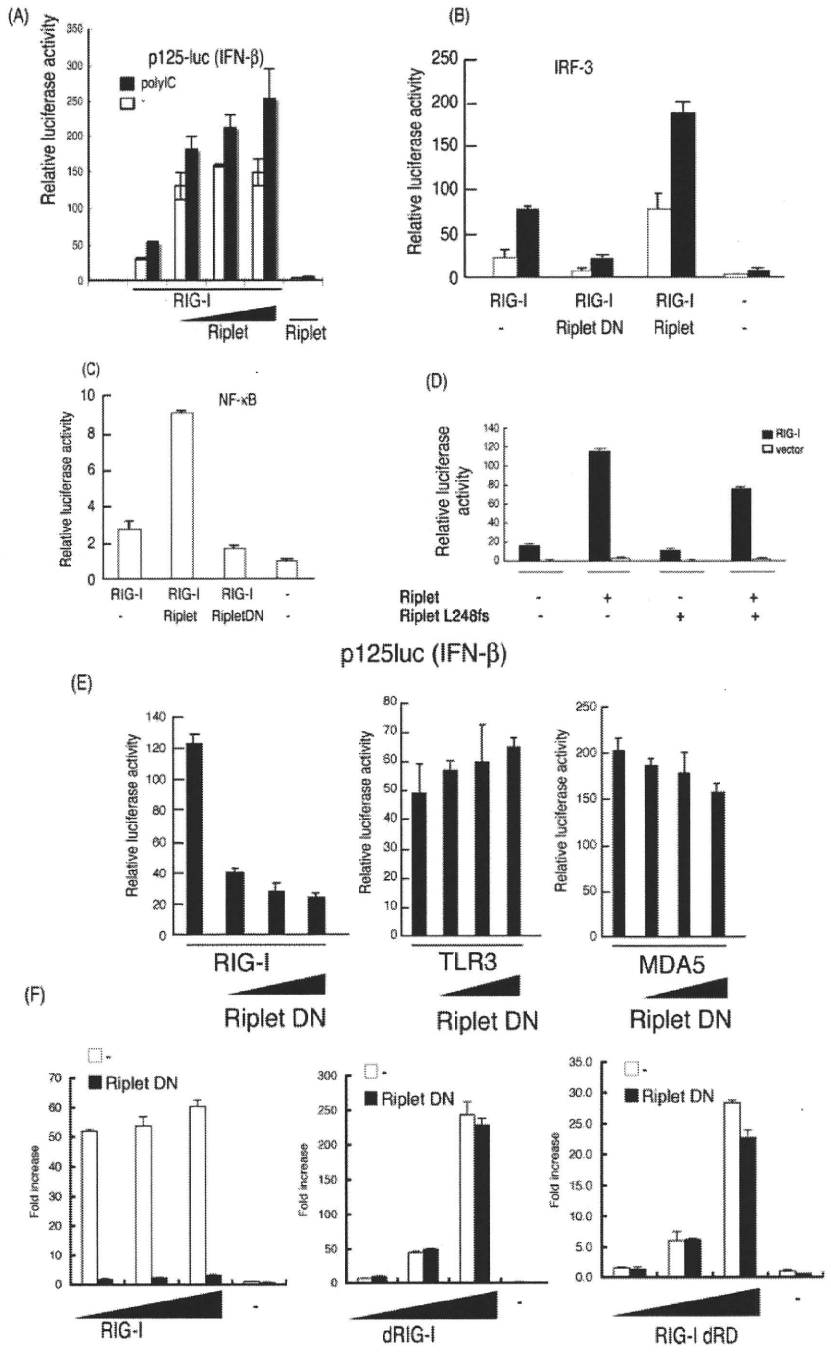

interaction of RIG-I with ZNF598 or RNF135 in HEK293FT cells by immunoprecipitation (data not shown). RNF135 was previously annotated by the genome project and was recently found to be a cause of a genetic disease, neurofibromatosis, although its protein function was unknown. We renamed the protein Riplet (RING finger protein leading to RIG-I activation) based on the following functional analyses. Riplet was most similar to TRIM25 (60.8% sequence homology), in particular between their RING finger domains PRY or SPRY (Fig. 1*B*). Phylogenetic analysis also supported the notion that Riplet was similar to TRIM25 (Fig. 1*C*). Thus, we hypothesized that, like TRIM25, Riplet is a ubiquitin ligase.

Expression of Riplet—RIG-I mRNA is induced by type I IFN or poly(I-C) stimulation in mammalian cells. Unlike RIG-I, however, Riplet mRNA was basally expressed in HeLa and primary-cultured MRC-5 cells irrespective of stimulation (Fig. 1*D* and data not shown). On the other hand, when we treated bone marrow-derived dendritic cells with poly(I-C), the basal level of Riplet mRNA was increased by the stimulation (Fig. 1*D*), suggesting that the regulatory mechanism of Riplet expression somewhat differs among cell types, and that Riplet is expressed before virus infection in some cell types. Next we performed Northern blotting of human tissue RNA. Riplet mRNA was detected as a single band of 2.4 kbp, which is slightly longer than the RNF135 cDNA sequence deposited in GenBank™ (accession number AB470605). Human *RIPLET* is expressed in human skeletal muscle, spleen, kidney, placenta, prostate, stomach, thyroid, and tongue and also weakly expressed in heart thymus, liver, and lung (Fig. 1*E*).

Riplet Enhances RIG-I-mediated IFN-β Induction—At first we characterized the role of Riplet in RIG-I-mediated IFN inducing signaling by reporter gene analyses. When RIG-I was expressed in HEK293 cells, reporter auto-activation was observed even in the absence of exogenous stimulation (Fig. 2*A*) as reported previously (25, 26). Stimulation with poly(I-C) further enhanced the promoter. Co-expression of Riplet with RIG-I potentiated activation of the IFN-β promoter, whereas expression of Riplet alone resulted in only marginal activation (Fig. 2*A*). Detection of endogenous IFN-β mRNA confirmed that Riplet enhanced RIG-I-mediated activation of IFN-β transcription (supplemental Fig. S1). The enhancing role of Riplet in IFN-β promoter activation was also supported by activation of IRF-3 and NF-κB by Riplet (Fig. 2, *B* and *C*). In contrast, expression of a Riplet partial fragment (Riplet-DN) (70–432 amino acids) that lacked the N-terminal RING finger domain reduced promoter activation (Fig. 2*E*). The Riplet-L249fs mutant protein, which was isolated from neurofibromatosis patients (27), did not increase the RIG-I-mediated promoter activation (Fig. 2*D*). These data indicate that Riplet augments RIG-I-mediated IFN-β promoter activation, and that both the RING finger domain and the C-terminal region encoding the SPRY and PRY motifs are important for its function. Riplet (residues 70–432) acted as a dominant-negative form (hereafter called Riplet-DN) (Fig. 2, *E* and *F, left panel*). This functional feature of Riplet-DN was confirmed in Fig. 2, *B* and *C*, and was later confirmed through RIG-I co-precipitation and ubiquitination analyses (see Fig. 5*C* and supplemental Fig. S4*C*). Expression of Riplet-DN did not reduce TLR3 or MDA5 signaling (Fig. 2*E*), suggesting that Riplet-DN is specific for RIG-I signaling. Interestingly, the Riplet-DN only partially suppressed the function of the C-terminal deleted RIG-I (dRD), which is a constitutively active form (Fig. 2*F, right panel*), and RIG-I CARD-like region (dRIG-I)-mediated signaling in high or low dose transfection of dRIG-I was barely inhibited by overexpression of Riplet-DN (Fig. 2*F, center panel*). These data suggest that Riplet requires the RIG-I C-terminal domain (RD) and partial helicase region to activate RIG-I signaling.

Endogenous Riplet Promotes the RIG-I Signaling—We performed Riplet knockdown by siRNA Riplet using Lipofectamine 2000 reagents, instead of FuGENE HD, to reveal the function of endogenous Riplet. Two siRNAs (Riplet siRNA and Riplet si-1) that target different sites of the Riplet mRNA and two control siRNAs were used for knockdown analyses. The two siRNA or control siRNA were co-transfected with HA-tagged Riplet expression vector into HEK293 cells, and after 48 h, cell lysate was prepared and analyzed by Western blotting with anti-HA antibody detecting Riplet. The two siRNAs targeting Riplet abolished exogenously expressed Ripelt-HA, but control siRNA did not (supplemental Fig. S3). Likewise, both Riplet siRNA and Riplet si-1 specifically down-regulate the level of endogenous Riplet mRNA (Fig. 3, *A* and *B*).

Using the siRNA, we examined whether Riplet knockdown reduces RIG-I signaling. As expected, RIG-I-mediated IFN-β promoter activation was reduced by Riplet siRNA or Riplet si-1 compared with control siRNA (Fig. 3, *A* and *B*), indicating that Riplet is required for full activation of the RIG-I signaling. Vesicular stomatitis virus (VSV) is a negative-stranded RNA virus that induces IFN-β production via RIG-I (3). Although the

FIGURE 2. **Riplet enhances IFN-β signaling mediated by RIG-I.** *A*, Riplet enhances the promoter activation by RIG-I. HEK293 cells were transfected with plasmids encoding empty vector, RIG-I (0.1 μg) and Riplet (0.025, 0.05, or 0.1 μg) together with p125-luc (IFN-β promoter) reporter plasmid in 24-well plates. 24 h after transfection, the cells were treated with mock or poly(I-C) (50 μg/ml) for 4 h as described under "Experimental Procedures," and then luciferase activities of cell lysates were measured. *Closed* or *open boxes* represent poly(I-C) or mock stimulation, respectively. *B*, to examine the activation of IRF-3, RIG-I (0.1 μg), Riplet (0.1 μg), and/or Riplet-DN (0.1 μg),expressing vectors were transfected into HEK293 cells with reporter plasmids, GAL4 fused IRF-3 (0.05 μg), and the p55 UASG-luc reporter gene (0.05 μg), in which luciferase reporter gene is fused downstream of GAL4 protein-binding site, and therefore activated IRF-3 promotes the transcription of luciferase reporter gene. The cells were stimulated with poly(I-C) as described above (34). The total amount of transfected DNA (0.5 μg/well) was kept constant by adding empty vector (pEF-BOS). *C*, HEK293 cells were transfected with RIG-I (0.1 μg), Riplet (0.1 μg), and/or Riplet-DN (0.1 μg) expressing vectors together with the NF-κB reporter plasmid (0.1 μg), and 24 h later, the luciferase activities of cell lysates were measured. *D*, Riplet-L248fs, which lacks the C-terminal region, did not enhance the activation at all. HEK293 cells were transfected with the plasmids expressing wild-type Riplet (0.1 μg) or Riplet-L248fs (0.1 μg) together with RIG-I expressing vector (0.1 μg) and p125-luc reporter (0.1 μg). 24 h after transfection, cell were stimulated with poly(I-C), and the luciferase activities of cell lysates were determined as described above. *E*, RIG-I (0.1 μg), MDA5 (0.1 μg), or TLR3 (0.1 μg) expressing vectors were transfected into HEK293 cells with the plasmid encoding the Riplet-DN fragment (0.1, 0.2, or 0.3 μg) in 24-well plates. After 24 h, the cells were stimulated with 50 μg of poly(I-C) for 4 h, and relative luciferase activities were determined. *F*, Riplet-DN (100 ng) was co-transfected with full-length RIG-I (0, 50, 100, or 200 ng), RIG-I CARD-like region (dRIG-I) (0, 50, 100, or 200 ng), or C-terminal deleted RIG-I (RIG-I dRD) (0, 50, 100, or 200 ng) into HEK293 cells in 24-well plate, and reporter gene assays were carried out.

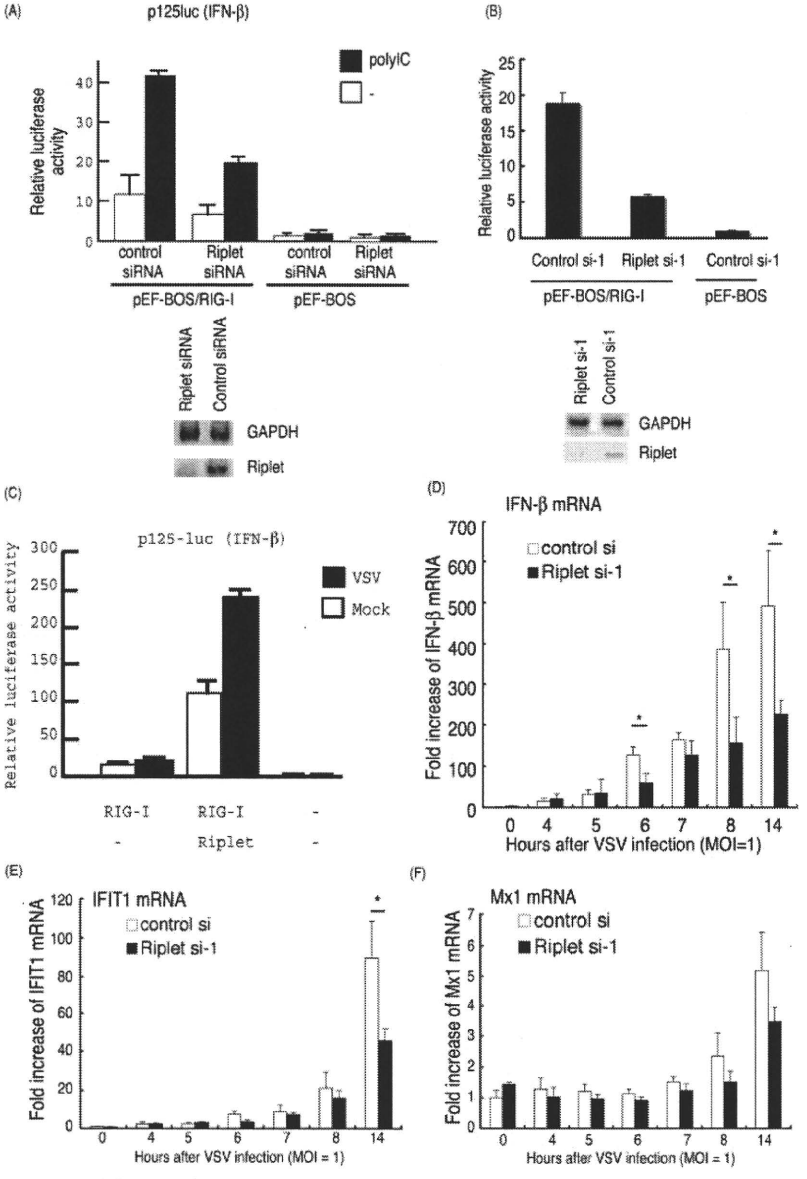

FIGURE 3. **Knockdown analyses of Riplet.** *A*, p125 luc reporter plasmid (0.1 μg), RIG-I expressing vector (0.1 μg), and Riplet siRNA or control siRNA (10 pmol), which were purchased from Funakoshi Co. Ltd., were transfected into HEK293 cells in a 24-well plate with Lipofectamine 2000, and 48 h after transfection, the cells were stimulated with poly(I-C) for 6 h, and the cell lysate was prepared, and luciferase activities were measured. RT-PCR was carried out using total RNA extracted from cells 48 h after transfection. *B*, p125 luc reporter plasmid (0.1 μg), RIG-I expressing vector (0.1 μg), and siRNA, Riplet si-1, or control si-1 (10 pmol), which were purchased from Applied Biosystems, were transfected into HEK293 cells with Lipofectamine 2000. 48 h after transfection, the cells were stimulated with poly(I-C) for 6 h. The cell lysate was prepared, and luciferase activities were measured. RT-PCR was carried out using total RNA extracted from cells 48 h after transfection. *C*, HEK293 cells were transfected with the plasmids expressing RIG-I (0.1 μg) and/or Riplet (0.1 μg) with p125 luc reporter plasmid (0.1 μg) in 24-well plates. After 24 h, the cells were infected with VSV (m.o.i. = 1) for 12 h. The luciferase activities of the cell lysates were measured. Expression of Riplet strongly enhanced IFN-β promoter activation by VSV through RIG-I. *D–F*, siRNA (control si- or Riplet si-1) were transfected into HEK293 cells, and after 48 h, the cells were infected with VSV at m.o.i. = 1. RNA was extracted at the indicated hours, and the quantitative PCR were carried out to detect the expression of IFN-β (*D*), IFIT-1 (*E*), or Mx1 (*F*) mRNA. *, $p < 0.05$. *GAPDH*, glyceraldehyde-3-phosphate dehydrogenase.

IFN-β promoter was only minimally activated by RIG-I in response to VSV (m.o.i. = 1) during the early phase of infection (<12 h), the activity was increased by RIG-I and Riplet (Fig. 3*C*). Riplet was silenced by siRNA and then VSV infected the cells. VSV-derived up-regulation of IFN-β mRNA was started around 6 h post-infection, and Riplet siRNA significantly suppressed the increase of IFN-β mRNA at 6 h (Fig. 3*D*). Because VSV infection is mainly sensed by RIG-I, this is consistent with the notion that Riplet promotes the RIG-I signaling. Other IFN-inducible genes, *IFIT1* and *MX1*, were expressed >8 h post-infection, and their expressions were also suppressed by Riplet siRNA (Fig. 3, *E* and *F*).

Riplet Exerts Protective Activity against Viral Infection—Next we examined the role of Riplet during viral infection. Riplet and/or RIG-I were transiently expressed in the human cells by FuGENE HD reagents, and then the cells were infected with VSV or poliovirus (a positive-stranded RNA virus). The viral titer of the supernatant was determined 24 h post-infection. Under our conditions, expression of RIG-I weakly inhibited VSV propagation. Co-expression of Riplet with RIG-I significantly suppressed VSV replication especially at low m.o.i., whereas Riplet alone did not suppress VSV (Fig. 4, *A* and *B*, *upper panel*). Therefore, a sufficient amount of RIG-I protein is required for Riplet to exert antivirus activity. This requirement of RIG-I is also observed in reporter gene analyses (Fig. 2). Under a similar setting, the antiviral effect of Riplet was marginally observed against poliovirus, which induces IFN-β largely via MDA5 (Fig. 4*B*, *lower panel*). To assess the importance of endogenous Riplet for antivirus effect of human cells, Riplet knockdown cells were infected with viruses. In Riplet knockdown cells, the VSV titer was consistently increased compared with the control ($p < 0.05$) (Fig. 4*C*, *left panel*). In addition, infection of Riplet knockdown cells with poliovirus resulted in only a slight increase in the poliovirus titer compared with the control ($p > 0.05$) (Fig. 4*C*, *right panel*). Because poliovirus is mainly recognized by MDA5 but not RIG-I, this marginal effect of Riplet on poliovirus infection was within expectation (3, 28).

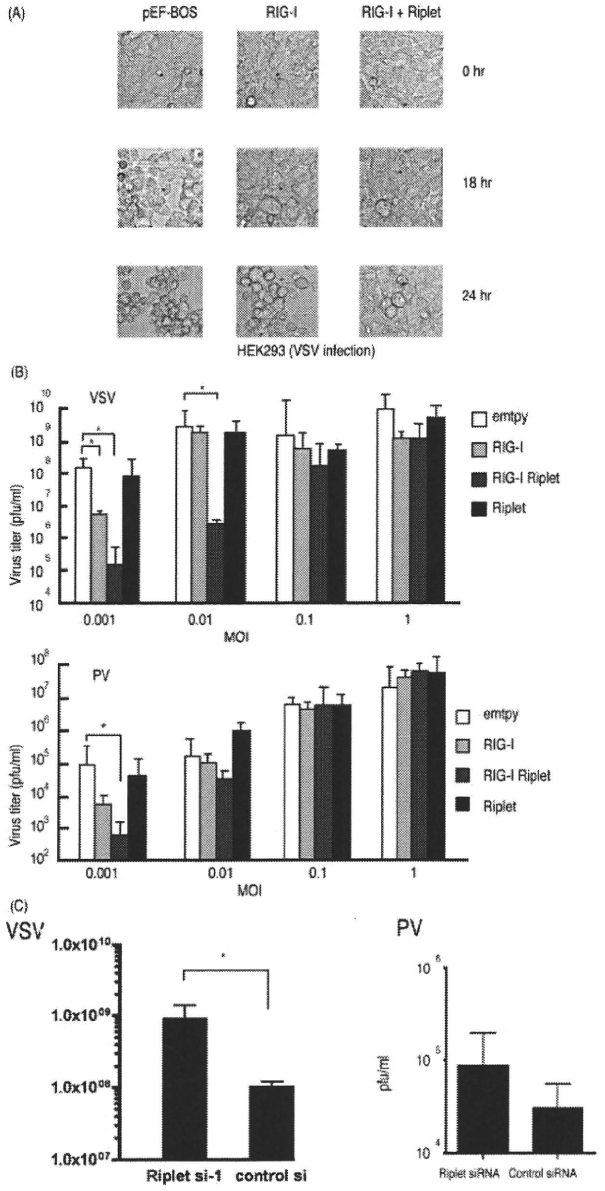

FIGURE 4. **Suppression of RNA viruses by Riplet.** *A*, HEK293 cells were transfected with RIG-I (0.1 μg) and/or Riplet (0.1 μg) expressing vectors. The total amount of transfected DNA (0.5 μg/well) in each well was kept constant by adding empty vector (pEF-BOS). 24 h after transfection, the cells were infected with VSV at m.o.i. = 0.1, and after 0, 18, or 24 h, CPE was observed by microscope. *B*, RIG-I (0.1 μg) and/or Riplet (0.1 μg) expressing plasmids were transfected to HEK293 cells in 24-well plates and incubated for 24 h. The total amount of transfected DNA (0.5 μg/well) in each well was kept constant by adding empty vector (pEF-BOS). The cells were infected with VSV (*upper panel*) or poliovirus (*PV*) (*lower panel*) at the indicated m.o.i. The viral titers in the culture media were measured 24 h after infection by plaque assay. *Error bars* represent standard deviation ($n = 3$). *, $p < 0.05$. *C*, control or Riplet knockdown HEK293 cells were infected with VSV (*left panel*) or poliovirus (*right panel*) at m.o.i. = 0.1. The viral titers in the culture media were measured 26 h after infection by plaque assays. Knockdown of Riplet induced higher VSV titers compared with control ($p < 0.05$), but the increase observed in poliovirus-infected Riplet knockdown cells was not significant ($p > 0.05$).

Riplet and Riplet-DN Bind the Helicase and RD Regions of RIG-I—Yeast two-hybrid analysis showed that a C-terminal region of Riplet bound to the C-terminal region of RIG-I. This cytoplasmic interaction between Riplet and RIG-I was confirmed by confocal microscopy in HeLa cells (supplemental Fig. S2). To further confirm the physical binding of Riplet to RIG-I in human cells, we carried out immunoprecipitation analyses. Full-length Riplet was co-immunoprecipitated with RIG-I (Fig. 5*B*), indicating that Riplet binds directly to RIG-I in human cells.

To determine the region responsible for the RIG-I-Riplet interaction, we constructed a RIG-I and Riplet deletion series as shown in Fig. 5*A*. Riplet-DN also bound to RIG-I (Fig. 5, *B* and *C*), indicating that the RING finger domain is dispensable for the RIG-I-Riplet interaction. This is consistent with the notion that the RING finger domain in ubiquitin ligase proteins is required for their interactions with ubiquitin-conjugating enzymes (29). Unlike TRIM25, Riplet and Riplet-DN failed to co-precipitate the two CARD domains of RIG-I (dRIG-I) (Fig. 5*D*). However, co-precipitation of the RIG-IC or RIG-RD fragments was observed (Fig. 5, *E* and *F*). RD-deleted RIG-I (RIG-I dRD) weakly associated with Riplet (Fig. 5*G*). Taken together, Riplet preferentially binds the RD and also weakly associates with the helicase region of RIG-I with its C terminus. Reporter gene analyses show that Riplet-DN only weakly suppresses RIG-I signaling and barely suppresses dRIG-I, which contains neither helicase nor RD region. Therefore, the physical interaction is correlated with the results of reporter activity.

Riplet Promotes Ubiquitination of RIG-I—Because Riplet shares 60% sequence similarity with TRIM25, we hypothesized that Riplet ubiquitinates RIG-I and that this modification leads to activation of RIG-I signaling. To test this hypothesis, we examined RIG-I ubiquitination. As expected, ubiquitination of RIG-I was increased by co-expression of Riplet under two different conditions (Fig. 6, *A* and *B*). The quantity of RIG-I ubiquitination was significantly high in the presence of Riplet (Fig. 6*C*). RIG-I ubiquitination was suppressed if Riplet was replaced with Riplet-DN (Fig. 6*D* and supplemental Fig. S4*C*). However, unlike TRIM25, Riplet binds to the C-terminal region of RIG-I. Therefore, we examined whether Riplet ubiquitinates the C-terminal region. We found that ubiquitination of RIG-IC was enhanced by Riplet expression (Fig. 6*E*). Both RIG-I dRD and RIG-I RD were also ubiquitinated by expression of Riplet (Fig. 6*F*; supplemental Fig. S4*A* and S5), suggesting that Riplet promotes ubiquitination of the helicase and RD domains of RIG-I in a manner distinct from TRIM25.

Ubiquitin is polymerized through its lysine residue. Lys-63-linked polyubiquitination is frequently observed in signal transduction pathways (30). In contrast, Lys-48-linked polyubiquitination usually leads to the degradation of protein through the proteasome. Indeed, TRIM25-mediated Lys-63-linked polyubiquitination activates the CARD-like region of RIG-I, and RNF125-mediated Lys-48-linked polyubiquitination leads to the degradation of RIG-I (23, 25). We used K48R or K63R mutated ubiquitin and found that K48R was incorporated normally into RIG-IC, whereas polyubiquitination was decreased by K63R (supplemental Fig. S4*B*). K63R mutation abolished RIG-I RD polyubiquitination by Riplet (Fig. 6*F*). These data

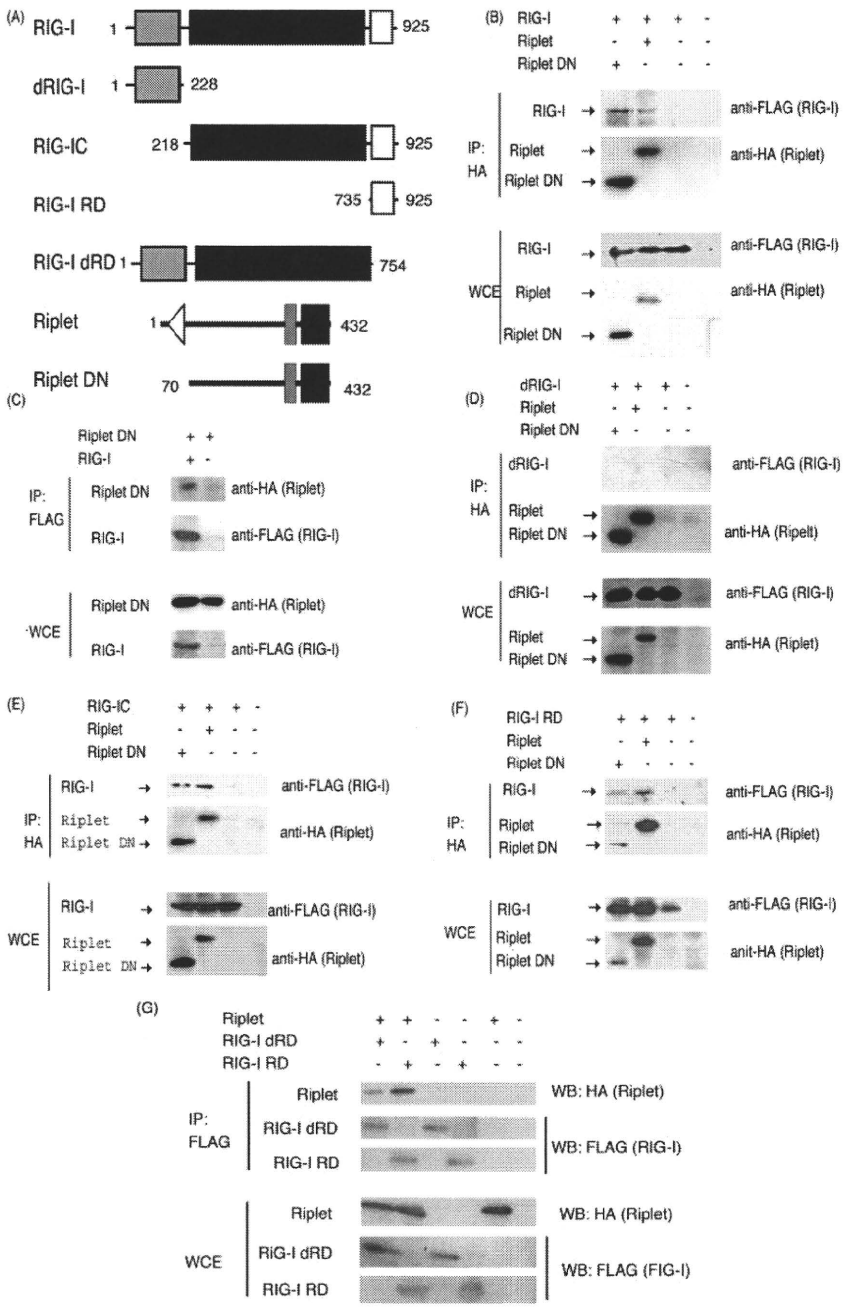

FIGURE 5. **Physical interaction of Riplet with RIG-I.** *A*, schematic representation of RIG-I or Riplet fragments used for immunoprecipitation analyses. *B*, HA-tagged Riplet (0.4 μg) or Riplet-DN (0.4 μg) were transfected into HEK293FT cells in a 6-well plate with FLAG-tagged RIG-I (0.4 μg). HA-tagged Riplet or Riplet-DN were immunoprecipitated (*IP*) with anti-HA antibodies, and samples were analyzed by Western blotting (*WB*) using an anti-FLAG or anti-HA antibody. The total amount of transfected DNA (2 μg/well) was kept constant by adding empty vector (pEF-BOS). *C*, HA-tagged Riplet-DN (0.4 μg) and FLAG-tagged RIG-I (0.4 μg) were transfected into HEK293FT cells in a 6-well plate. RIG-I was immunoprecipitated with anti-FLAG antibody, and samples were analyzed by Western blotting using an anti-FLAG or -HA antibody. The total amount of transfected DNA (2 μg/well) was kept constant by adding empty vector (pEF-BOS). *D–F*, interaction of HA-tagged Riplet or Riplet-DN with FLAG-tagged dRIG-I (*D*), RIG-IC (*E*), or RIG-I RD (*F*) was examined using immunoprecipitation assays. The proteins were expressed in HEK293FT cells, and HA-tagged Riplet was immunoprecipitated with anti-HA antibody, and samples were analyzed by Western blotting using an anti-FLAG or -HA antibody. *G*, FLAG-tagged RIG-I RD (0.4 μg) or RIG-I dRD (0.4 μg) was transfected with HA-tagged Riplet (0.4 μg) into HEK293 FT cells in a 6-well plate, and 24 h after transfection, immunoprecipitation was performed with anti-FLAG antibody and analyzed by Western blotting. The total amount of transfected DNA (2 μg/well) was kept constant by adding empty vector (pEF-BOS). *WCE*, whole cell extract.

indicates that Riplet mediates Lys-63-linked polyubiquitination of the RIG-I C-terminal helicase and RD region. Because Riplet-DN reduced the RIG-I-mediated signaling, we examined whether Riplet-DN reduced the RIG-I ubiquitination. As expected, Riplet-DN reduced RIG-I ubiquitination (Fig. 6*D* and supplemental Fig. S4*C*). These ubiquitination assay data are consistent with the notion that Riplet-mediated Lys-63-linked polyubiquitination of RIG-I is required for full activation of RIG-I signaling.

We tried to determine the ubiquitination sites of RIG-I using Lys-to-Ala (KA)-converting mutants. RIG-I has 25 Lys residues in its C-terminal region. These Lys residues of RIG-I were in turn mutated to Ala, and the degree of ubiquitination and IFN-β-inducing activity were determined with each mutant. RIG-I-mediated IFN-β promoter activation was normally augmented by co-expression of Riplet and 3KA RIG-I. Co-expression of Riplet and 5KA, however, and the ubiquitination level of RIG-I and IFN-β-inducing activity were simultaneously decreased (Fig. 7, *A* and *C*). Riplet-dependent augmentation of IFN-β promoter activation was largely suppressed when RIG-I was replaced with 5KA RIG-I (Fig. 7*B*). Therefore, Lys-849 and Lys-851 of RIG-I were crucial for RIG-I ubiquitination by Riplet. The results confirmed the importance of ubiquitination of specific Lys residues in the C-terminal region of RIG-I and for RIG-I-mediated IFN-β induction.

DISCUSSION

RIG-I plays a central role in the recognition of cytoplasmic viral RNA and is regulated by modification by small modifier ubiquitin or ubiquitin-like protein, ISG15. TRIM25 mediates Lys-63-linked polyubiquitination, which is essential for RIG-I activation (23), and RNF125 mediates Lys-48-linked polyubiquitination (25). RIG-I also harbors ISG15 modification, although the role of ISG15 modification *in vivo* remains to be deter-

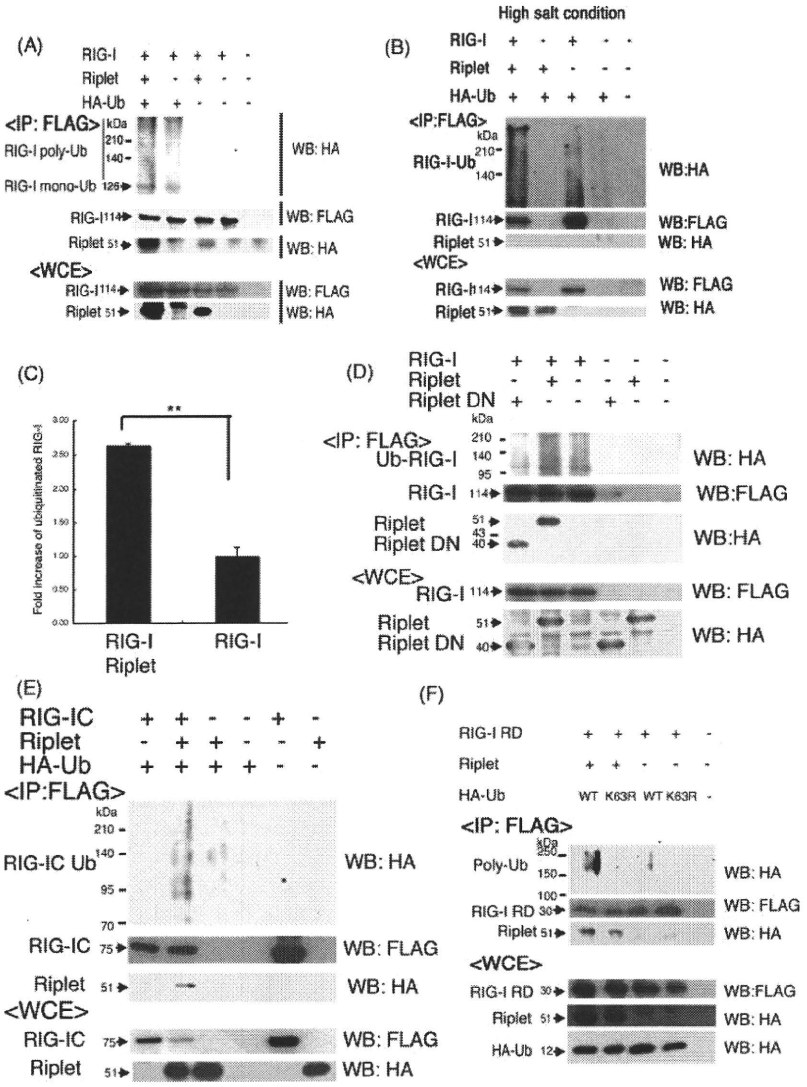

FIGURE 6. **Ubiquitination of RIG-I by Riplet.** *A* and *B*, FLAG-tagged RIG-I (0.4 μg), Riplet (0.4 μg), and HA-tagged ubiquitin (0.4 μg) expressing vectors were transfected into HEK293FT cells in 6-well plates. The total amount of transfected DNA (2 μg/well) was kept constant by adding empty vector (pEF-BOS). FLAG-tagged RIG-I was immunoprecipitated (*IP*) using an anti-FLAG antibody, and washed with the buffer containing 150 mM NaCl (*A*) or 1 M NaCl (*B*). The immunoprecipitates were separated with 8% acrylamide gel and analyzed by Western blotting (*WB*) using antibodies against HA tag (ubiquitin) or FLAG (RIG-I). Riplet was co-immunoprecipitated with FLAG-tagged RIG-I in *A* but could not co-immunoprecipitate in *B* because of high salt condition. Expression of Riplet enhanced the ubiquitination of RIG-I. Different gel conditions were employed in *A* and *B*. *C*, ubiquitinated RIG-I was quantitated with NIH image software. **, $p < 0.01$. *D*, FLAG-tagged RIG-I (0.4 μg) was transfected into HEK293 FT cells in a 6-well plate with HA-tagged Riplet (0.4 μg) or Riplet-DN (0.4 μg) and HA-tagged ubiquitin, and immunoprecipitation was carried out with anti-FLAG antibody. The total amount of transfected DNA (2 μg/well) was kept constant by adding empty vector (pEF-BOS). The samples were analyzed with 10% acrylamide gel to clearly separate Riplet from Riplet-DN and stained by Western blotting. *E*, ubiquitination of RIG-IC was also promoted by Riplet expression. HEK293FT cells were transfected with the plasmids encoding RIG-IC (0.4 μg), Riplet (0.4 μg), and/or HA-tagged ubiquitin (0.4 μg) in a 6-well plate, and 24 h after transfection, cell lysates were prepared. The total amount of transfected DNA (2 μg/well) was kept constant by adding empty vector (pEF-BOS). FLAG-tagged RIG-ICs were immunoprecipitated with anti-FLAG antibodies, and the proteins were analyzed by Western blotting. *F*, Ub-K63R are HA-tagged ubiquitin in which the lysine 3 residues were substituted with arginine. The HA-tagged Ub-K63 expressing vectors (1.2 μg), FLAG-tagged RIG-IC (0.4 μg), and/or Riplet (0.4 μg) were transfected into HEK293FT cells in 6-well plates and analyzed as shown in *A–D*. The total amount of transfected DNA (2 μg/well) was kept constant by adding empty vector (pEF-BOS). Ub-K63R was not incorporated into polyubiquitin chain of RIG-I RD. *WCE*, whole cell extract.

mined (21, 22, 31). Although Riplet and TRIM25 share 60% sequence similarity, the ubiquitination of RIG-I by Riplet is distinct from that by TRIM25; Riplet ubiquitinates the C-terminal region of RIG-I, whereas TRIM25 ubiquitinates its CARD-like region. These findings are also supported by the fact that neither Riplet nor Riplet-DN promoted or inhibited the activation of the IFN-β promoter by expression of the RIG-I CARD-like region (data not shown). It has been reported that ubiquitination of the CARD-like region of RIG-I by TRIM25 is critical for RIG-I-IPS-1 signaling (23). However, how this CARD ubiquitination is essential for activation of IPS-1 by RIG-I remains undetermined. Here we emphasize the importance of RIG-I C-terminal ubiquitination for IFN-β induction and the antiviral response. Because the C-terminal RD region inhibits the IFN inducing activity of the CARD-like region of RIG-I, it is reasonable that RIG-I C-terminal ubiquitination by Riplet inhibits the conversion from the active to inactive form of RIG-I protein after binding to viral RNA. This initial stabilization of RIG-I via ubiquitination by Riplet would provide a sufficient structure for RIG-I to maintain the accessibility to TRIM25 and facilitate TRIM25-mediated ubiquitination of the CARD-like region of RIG-I, which may lead to potential activation of IPS-1.

RIG-I is an IFN-inducible RNA helicase that is expressed at extremely low levels in resting cells (6). Initial penetration of viruses allows generation of 5′-triphosphate RNA and/or double strand RNA followed by induction of IFN-β production. This early response to viral infections triggers up-regulation of RIG-I/MDA5 and TLR3, leading to robust IFN-β production (3, 32, 33). We favor the interpretation of our present findings that during the early stages of viral infection with trace amounts of RIG-I and viral RNAs, Riplet helps host cells rearrange RIG-I conformation to activate IPS-1. This issue will need further proof because it is difficult to

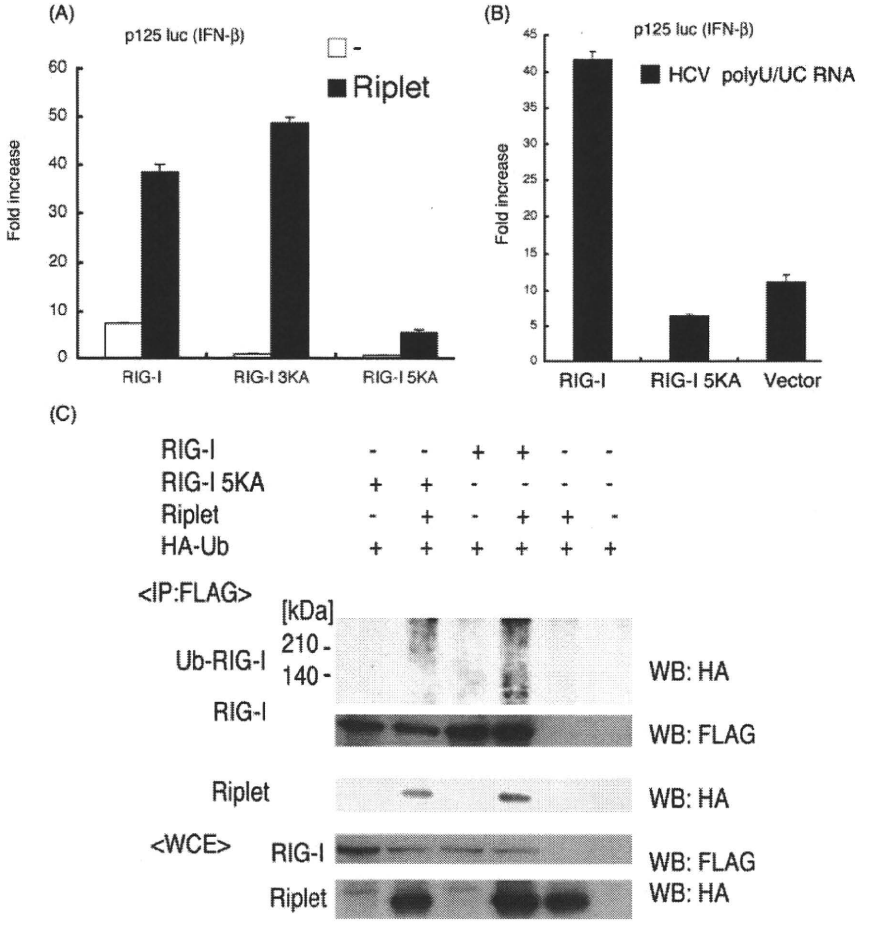

FIGURE 7. **The C-terminal two lysine residues of RIG-I are important for ubiquitination by Riplet.** *A*, RIG-I C-terminal lysine residues were substituted with alanine. RIG-I 3KA mutant protein harbors the triple mutations, K888A, K907A, and K909A. The five lysine residues, Lys-849, Lys-851, Lys-888, Lys-907, and Lys-909, were replaced with alanine in RIG-I 5KA mutant. The plasmid carrying wild-type (100 ng/well), RIG-I 3KA (100 ng/well), RIG-I 5KA (100 ng), or Riplet (100 ng) were transfected into HEK293 cells in a 24-well plate together with p125 luc reporter plasmid (100 ng/well). The amount of transfected DNA was kept constant by adding empty vector. After 24 h, the luciferase activities were measured. *B*, wild-type RIG-I (100 ng), RIG-I 5KA mutant (100 ng), or empty vector (100 ng) was transfected into HEK293 cells in a 24-well plate together with p125 luc reporter plasmids and HCV 3′-untranslated region poly(U/UC) RNA (25 ng), which is synthesized in *in vitro* transcription by T7 RNA polymerase. The amount of transfected DNA was kept constant by adding empty vector. 24 h after transfection, luciferase activities were measured. RIG-I 5KA mutant hardly responded to poly(U/UC) RNA. *C*, to observe the ubiquitinated RIG-I more clearly, we used 800 ng/well of Riplet and HA-Ub expression vector for the following transfection. HEK293FT cells in a 6-well plate were transfected with the plasmids encoding RIG-I (400 ng/well), RIG-I 5KA (400 ng/well), Riplet (800 ng/well), and/or HA-Ub (800 ng/well). The total amount of DNA was kept constant by adding the empty vector. 24 h after the transfection, the cell lysates were prepared, and the immunoprecipitation was carried out using anti-FLAG antibodies. The immunoprecipitates were analyzed by Western blotting with anti-HA or FLAG antibodies.

visualize RNRs and viral RNAs in the early infection stage and to understand the mechanisms that allow viruses to uncoat into naked viral RNA and to replicate.

We have provided several lines of evidence indicating that Riplet complements RIG-I-mediated IFN-β induction upon viral infection by both Riplet siRNA and overexpression analyses. The C-terminal lysines (849 and 851) of RIG-I are critical for Riplet-mediated RIG-I ubiquitination. However, our data indicate that Riplet alone was unable to induce IFN-β production and essentially required RIG-I to confer IFN-β induction. Furthermore, Riplet is not ubiquitously distributed over the organs tested. Ubiquitination of RIG-I induced by poly(I-C) or viruses was accelerated in cells pre-transfected with Riplet. Hence, Riplet works case-sensitive to up-regulate RIG-I antiviral activity predominantly in some organs. The physiological meaning of this response will be clarified by knock-out study.

Unexpectedly, the siRNA experiments were not robust with regard to VSV replication. Possible explanations for this are as follows: 1) the degree of gene silencing is not so profound that the proteins remain in the cells; 2) there are a number of virus-mediated IFN-inducing pathways capable of compensating each other, so that disruption of one factor does not cause a profound effect on VSV replication. Furthermore, in VSV-infected Riplet-knockdown cells, IFN-β levels were reduced even at m.o.i. = 1 (Fig. 3*D*), and accordingly, virus susceptibility was increased at m.o.i. = 0.1 (Fig. 4*C*), whereas in Riplet-overexpressing cells, antiviral activity was observed only at low m.o.i. (Fig. 4*B*). We used different transfection reagents and cell conditions in the knockdown and overexpression experiments to obtain high transfection efficiency in each. These conditional differences in knockdown and overexpression analyses might cause part of the discrepancy between the two results on Riplet antiviral activity. Another possibility to explain the apparent inconsistencies between overexpression and knockdown analyses is that high amounts of Riplet efficiently activate the RIG-I signaling, but low amounts are insufficient for RIG-I activation in high m.o.i.-infecting human cells. High amounts of Riplet with overexpressed RIG-I would confer the ability on cells to respond to very low amounts of VSV as observed in the low m.o.i. experiments. Again, *riplet* knock-out mice would reveal whether it is absolutely required for potential RIG-I activation.

How viral RNAs select RIG-I rather than dicers or the translation machinery is also unknown. During natural infection it is likely that the number of the initial invading virions would be at most several copies/cell. Uncoated viral RNA may assemble a complex consisting of viral and host molecules required for replication. We assume that cells are equipped with various

molecular arms to sensitively detect viral RNA. The molecular complexes sensing viral RNA may not be so simple that we will be able to identify more molecules than Riplet as enhancers for integral RNA recognition. In either case, yeast screening will be a good strategy to pick up such proteins in other RNA recognition systems. A molecular switch selecting IFN induction by virus RNA will then be clarified.

We show that the ubiquitination sites targeted by Riplet are the helicase and RD domains of RIG-I but not its CARD-like domains in contrast to TRIM25. Riplet may be a complement factor of the reported TRIM25 function for RIG-I activation (23). A previous report (25) failed to polyubiquitinate the RIG-I protein by TRIM25 alone. If Riplet were added to TRIM25 for RIG-I ubiquitination in the previous study, Riplet would have enabled TRIM25 to polyubiquitinate the RIG-I CARD-like region. Further studies using TRIM25 and Riplet will be required to clarify this point.

Based on our results, we propose that RIG-I-like receptors form a molecular complex that efficiently recognizes low copy numbers of viral RNA. Riplet is implicated in the RIG-I complex to enhance viral RNA response in some organs. In this context, MDA5-associated molecules might also exist in the cytoplasm to augment IFN output. Although MDA5 possesses the RD domain, it fails to recruit Riplet (data not shown) or augment IFN-β-induction in conjunction with Riplet (Fig. 2*E*). Because RLR-associated molecules naturally reside in cells and facilitate inhibition of low dose viral infection until RLRs become expressed, they may be useful therapeutic targets for an early phase antiviral immunotherapy.

Acknowledgments—We thank Dr. M. Sasai in our laboratory for technical instructions for assay of RIG-I functions and Drs. K. Shimotohno (Keio University), T. Taniguchi (University of Tokyo), and T. Fujita (Kyoto University) for their critical discussions.

REFERENCES

1. Takeuchi, O., and Akira, S. (2008) *Curr. Opin. Immunol.* **20,** 17–22
2. Honda, K., Takaoka, A., and Taniguchi, T. (2006) *Immunity* **25,** 349–360
3. Kato, H., Takeuchi, O., Sato, S., Yoneyama, M., Yamamoto, M., Matsui, K., Uematsu, S., Jung, A., Kawai, T., Ishii, K. J., Yamaguchi, O., Otsu, K., Tsujimura, T., Koh, C. S., Reis e Sousa, C., Matsuura, Y., Fujita, T., and Akira, S. (2006) *Nature* **441,** 101–105
4. Venkataraman, T., Valdes, M., Elsby, R., Kakuta, S., Caceres, G., Saijo, S., Iwakura, Y., and Barber, G. N. (2007) *J. Immunol.* **178,** 6444–6455
5. Yoneyama, M., Kikuchi, M., Matsumoto, K., Imaizumi, T., Miyagishi, M., Taira, K., Foy, E., Loo, Y. M., Gale, M., Jr., Akira, S., Yonehara, S., Kato, A., and Fujita, T. (2005) *J. Immunol.* **175,** 2851–2858
6. Yoneyama, M., Kikuchi, M., Natsukawa, T., Shinobu, N., Imaizumi, T., Miyagishi, M., Taira, K., Akira, S., and Fujita, T. (2004) *Nat. Immunol.* **5,** 730–737
7. Hornung, V., Ellegast, J., Kim, S., Brzozka, K., Jung, A., Kato, H., Poeck, H., Akira, S., Conzelmann, K. K., Schlee, M., Endres, S., and Hartmann, G. (2006) *Science* **314,** 994–997
8. Pichlmair, A., Schulz, O., Tan, C. P., Naslund, T. I., Liljestrom, P., Weber, F., and Reis e Sousa, C. (2006) *Science* **314,** 997–1001
9. Saito, T., Hirai, R., Loo, Y. M., Owen, D., Johnson, C. L., Sinha, S. C., Akira, S., Fujita, T., and Gale, M., Jr. (2007) *Proc. Natl. Acad. Sci. U. S. A.* **104,** 582–587
10. Kawai, T., Takahashi, K., Sato, S., Coban, C., Kumar, H., Kato, H., Ishii, K. J., Takeuchi, O., and Akira, S. (2005) *Nat. Immunol.* **6,** 981–988
11. Meylan, E., Curran, J., Hofmann, K., Moradpour, D., Binder, M., Bartenschlager, R., and Tschopp, J. (2005) *Nature* **437,** 1167–1172
12. Seth, R. B., Sun, L., Ea, C. K., and Chen, Z. J. (2005) *Cell* **122,** 669–682
13. Xu, L. G., Wang, Y. Y., Han, K. J., Li, L. Y., Zhai, Z., and Shu, H. B. (2005) *Mol. Cell* **19,** 727–740
14. Rothenfusser, S., Goutagny, N., DiPerna, G., Gong, M., Monks, B. G., Schoenemeyer, A., Yamamoto, M., Akira, S., and Fitzgerald, K. A. (2005) *J. Immunol.* **175,** 5260–5268
15. Loo, Y. M., Fornek, J., Crochet, N., Bajwa, G., Perwitasari, O., Martinez-Sobrido, L., Akira, S., Gill, M. A., Garcia-Sastre, A., Katze, M. G., and Gale, M., Jr. (2008) *J. Virol.* **82,** 335–345
16. Komuro, A., and Horvath, C. M. (2006) *J. Virol.* **80,** 12332–12342
17. McWhirter, S. M., Tenoever, B. R., and Maniatis, T. (2005) *Cell* **122,** 645–647
18. Saha, S. K., Pietras, E. M., He, J. Q., Kang, J. R., Liu, S. Y., Oganesyan, G., Shahangian, A., Zarnegar, B., Shiba, T. L., Wang, Y., and Cheng, G. (2006) *EMBO J.* **25,** 3257–3263
19. Kayagaki, N., Phung, Q., Chan, S., Chaudhari, R., Quan, C., O'Rourke, K. M., Eby, M., Pietras, E., Cheng, G., Bazan, J. F., Zhang, Z., Arnott, D., and Dixit, V. M. (2007) *Science* **318,** 1628–1632
20. Lin, R., Yang, L., Nakhaei, P., Sun, Q., Sharif-Askari, E., Julkunen, I., and Hiscott, J. (2006) *J. Biol. Chem.* **281,** 2095–2103
21. Zhao, C., Denison, C., Huibregtse, J. M., Gygi, S., and Krug, R. M. (2005) *Proc. Natl. Acad. Sci. U. S. A.* **102,** 10200–10205
22. Arimoto, K., Konishi, H., and Shimotohno, K. (2008) *Mol. Immunol.* **45,** 1078–1084
23. Gack, M. U., Shin, Y. C., Joo, C. H., Urano, T., Liang, C., Sun, L., Takeuchi, O., Akira, S., Chen, Z., Inoue, S., and Jung, J. U. (2007) *Nature* **446,** 916–920
24. Urano, T., Saito, T., Tsukui, T., Fujita, M., Hosoi, T., Muramatsu, M., Ouchi, Y., and Inoue, S. (2002) *Nature* **417,** 871–875
25. Arimoto, K., Takahashi, H., Hishiki, T., Konishi, H., Fujita, T., and Shimotohno, K. (2007) *Proc. Natl. Acad. Sci. U. S. A.* **104,** 7500–7505
26. Sasai, M., Shingai, M., Funami, K., Yoneyama, M., Fujita, T., Matsumoto, M., and Seya, T. (2006) *J. Immunol.* **177,** 8676–8683
27. Douglas, J., Cilliers, D., Coleman, K., Tatton-Brown, K., Barker, K., Bernhard, B., Burn, J., Huson, S., Josifova, D., Lacombe, D., Malik, M., Mansour, S., Reid, E., Cormier-Daire, V., Cole, T., and Rahman, N. (2007) *Nat. Genet.* **39,** 963–965
28. Barral, P. M., Morrison, J. M., Drahos, J., Gupta, P., Sarkar, D., Fisher, P. B., and Racaniello, V. R. (2007) *J. Virol.* **81,** 3677–3684
29. Seol, J. H., Feldman, R. M., Zachariae, W., Shevchenko, A., Correll, C. C., Lyapina, S., Chi, Y., Galova, M., Claypool, J., Sandmeyer, S., Nasmyth, K., Deshaies, R. J., Shevchenko, A., and Deshaies, R. J. (1999) *Genes Dev.* **13,** 1614–1626
30. Pickart, C. M. (2004) *Cell* **116,** 181–190
31. Kim, M. J., Hwang, S. Y., Imaizumi, T., and Yoo, J. Y. (2008) *J. Virol.* **82,** 1474–1483
32. Alexopoulou, L., Holt, A. C., Medzhitov, R., and Flavell, R. A. (2001) *Nature* **413,** 732–738
33. Tanabe, M., Kurita-Taniguchi, M., Takeuchi, K., Takeda, M., Ayata, M., Ogura, H., Matsumoto, M., and Seya, T. (2003) *Biochem. Biophys. Res. Commun.* **311,** 39–48
34. Yoneyama, M., Suhara, W., Fukuhara, Y., Fukuda, M., Nishida, E., and Fujita, T. (1998) *EMBO J.* **17,** 1087–1095

Biochemical and Biophysical Research Communications 395 (2010) 565–571

Contents lists available at ScienceDirect

Biochemical and Biophysical Research Communications

journal homepage: www.elsevier.com/locate/ybbrc

Biological properties of purified recombinant HCV particles with an epitope-tagged envelope

Hitoshi Takahashi [a,b], Daisuke Akazawa [a,b], Takanobu Kato [a], Tomoko Date [a], Masayuki Shirakura [a,b], Noriko Nakamura [b], Hidenori Mochizuki [b], Keiko Tanaka-Kaneko [c], Tetsutaro Sata [c], Yasuhito Tanaka [d], Masashi Mizokami [e], Tetsuro Suzuki [a], Takaji Wakita [a,*]

[a] Department of Virology II, National Institute of Infectious Diseases, Tokyo, Japan
[b] Toray Industries, Inc., Kanagawa, Japan
[c] Department of Pathology, National Institute of Infectious Diseases, Tokyo, Japan
[d] Department of Clinical Molecular Informative Medicine, Nagoya City University Graduate School of Medicine, Nagoya, Japan
[e] Research Center for Hepatitis & Immunology, Kohnodai Hospital, International Medical Center of Japan, Chiba, Japan

ARTICLE INFO

Article history:
Received 3 April 2010
Available online 23 April 2010

Keywords:
Hepatitis C virus
Envelope protein
Purification
Particle
Vaccine

ABSTRACT

To establish a simple system for purification of recombinant infectious hepatitis C virus (HCV) particles, we designed a chimeric J6/JFH-1 virus with a FLAG (FL)-epitope-tagged sequence at the N-terminal region of the E2 hypervariable region-1 (HVR1) gene (J6/JFH-1/1FL). We found that introduction of an adaptive mutation at the potential *N*-glycosylation site (E2N151K) leads to efficient production of the chimeric virus. This finding suggests the involvement of glycosylation at Asn within the envelope protein(s) in HCV morphogenesis.

To further analyze the biological properties of the purified recombinant HCV particles, we developed a strategy for large-scale production and purification of recombinant J6/JFH-1/1FL/E2N151K. Infectious particles were purified from the culture medium of J6/JFH-1/1FL/E2N151K-infected Huh-7 cells using anti-FLAG affinity chromatography in combination with ultrafiltration. Electron microscopy of the purified particles using negative staining showed spherical particle structures with a diameter of 40–60 nm and spike-like projections. Purified HCV particle-immunization induced both an anti-E2 and an anti-FLAG antibody response in immunized mice. This strategy may contribute to future detailed analysis of HCV particle structure and to HCV vaccine development.

1. Introduction

The hepatitis C virus (HCV) causes chronic hepatitis, liver cirrhosis and hepatocellular carcinoma [1]. HCV is a positive strand RNA virus belonging to the *Hepacivirus* genus in the Flaviviridae family. The HCV genome consists of about 9600 nucleotides and contains three regions: a 5′ non-coding region of 341 nucleotides containing the sequence for the IRES structure, a coding region of about 9000 nucleotides, which encodes about 10 viral proteins, and a 3′ non-coding region of about 200 nucleotides depending on the size of the poly-uridylate track within this region [2,3].

The main therapy for HCV is treatment with pegylated-interferon and rivabirin. However, these agents show little effect in patients that have a high titer of HCV RNA, genotype 1. Thus, it is necessary to develop new, more effective therapies and preventive treatments to counteract HCV infection. As yet, no preventive vaccine is available for HCV. A recombinant HCV vaccine based on the viral envelope protein E1/E2 has been reported that generated neutralizing antibodies (nAb) in animals [4]. These nAbs were capable of limiting HCV pseudoparticles (HCVpp) and HCV cell culture (HCVcc) infection.

Recently, a genotype 2a strain of HCV named JFH-1 was discovered. This strain can efficiently replicate in the Huh-7 cell line [5], and an *in vitro* culture system of infectious HCV has also been successfully developed using the JFH-1 genome [6–8]. The JFH-1 viral production system is expected to become a powerful tool for HCV vaccine development. In this study, we developed a simple strategy for purification of recombinant HCV particles from the media of infected Huh-7 cells for structural analysis and for vaccine development using the JFH-1 genome.

2. Materials and methods

2.1. Plasmids

Plasmid pJ6/JFH-1 was generated from pJFH-1 by replacement of the 5′ untranslated region with the p7 region of J6 [9]. The

* Corresponding author. Address: Department of Virology II, National Institute of Infectious Diseases, 1-23-1 Toyama, Shinjuku, Tokyo 162-8640, Japan. Fax: +81 3 5285 1161.
E-mail address: wakita@nih.go.jp (T. Wakita).

0006-291X/$ - see front matter © 2010 Elsevier Inc. All rights reserved.
doi:10.1016/j.bbrc.2010.04.081

plasmids pJ6/JFH-1/1FL and pJ6/JFH-1/3FL were constructed by introduction of a single (DYKDDDDKGGG) or triple (DYKDHDG-DYKDHDIDYKDDDDKGGG) FLAG-tag sequence, respectively, into pJ6/JFH-1, which replaced part of the E2 HVR1 (amino acids 394–400) region. These two plasmids were then modified by introduction of a Lys residue to replace the Asn at amino acid position 151 of the E2 sequence, creating pJ6/JFH-1/1FL/E2N151K and pJ6/JFH-1/3FL/E2N151K, respectively.

The J6E2 gene (codons 1490–2500) was generated by PCR amplification from pJ6CF. The sense and antisense primers used were: 5′-CACAAGCTTCGCACCCATACTGTTGGGG-3′ and 5′-ACAGGATCCCAT-CGGACGATGTATTTTGTG-3′, respectively. For cloning purposes, HindIII or BamHI sites (underlined) were added to the primers. The amplified DNA was digested and inserted into p3XFLAG-CMV-13 (SIGMA, Saint Louis, MO).

The plasmid CDM-J6E2Fc encodes the J6E2 sequence downstream of the preprotrypsin leader sequence. pCDM-J6E2Fc was digested with SacI and BamHI, and the DNA fragment containing the preprotrypsin leader and J6E2 sequence was inserted into pCD4Rg (a kind gift from Dr. Brian Seed, Harvard Medical School) from which the SacI–BamHI fragment containing the CD4 gene was removed. This ligation resulted in the creation of a plasmid encoding a fusion gene of E2 and human IgG1-Fc.

2.2. Cell culture

The human hepatoma cell line, Huh-7, was maintained in DMEM supplemented with 10% FBS at 37 °C in a 5% CO_2 incubator.

2.3. In vitro synthesis of HCV RNA and RNA transfection of Huh cells

HCV RNA was synthesized from the plasmids described above *in vitro* using a MEGAscript T7 kit (Ambion, Austin, TX). Synthesized HCV RNA was then electroporated into cells as previously described [10]. The transfected cells were transferred onto 100-mm culture dishes containing culture medium.

2.4. Quantification of HCV core protein and RNA

The HCV core protein in cell culture supernatants or in purified HCV samples was quantified by enzyme immunoassay using a HCV core ELISA kit (Ortho Clinical Diagnostics). HCV RNA in purified HCV samples was quantified by RTD-PCR as previously described [11].

2.5. Deglycosylation with PNGase F

For deglycosylation reactions, the Enzymatic In-Solution N-Deglycosylation kit (Sigma) was used according to the manufacturer's instructions. Briefly, lysates of passaged cells were incubated for 10 min at 100 °C in denaturation buffer and then in the presence of PNGase F enzyme for 1 h at 37 °C. These samples were analyzed by Western blotting as described below using anti-FLAG (SIGMA) and anti-GAPDH (CHEMICON, Temecula, CA) antibodies.

2.6. Sequence analysis

The cDNAs of the HCV genome were synthesized from total RNA isolated from HCV RNA-transfected cells [5]. These cDNA were subsequently amplified using DNA polymerase (*TaKaRa LA Taq*, Takara, Shiga, Japan). The sequence of the amplified DNA was determined by the 3130 Genetic Analyzer (Applied Biosystems, Foster city, CA).

2.7. Purification of recombinant HCV particles

Culture supernatants from Huh-7 cells transfected with FLAG-tagged HCV RNA were harvested. The medium was concentrated by ultrafiltration using the pellicon-2 300 system (Millipore, Bedford, MA) and was subjected to affinity chromatography using an Anti-FLAG M2 affinity gel (Sigma). Virus particles were eluted using the 3×FLAG Peptide (Sigma) and were concentrated by ultracentrifugation for 2 h at 50,000 rpm at 4 °C.

2.8. Determination of the viral infectious titer

The infectious titer was determined by the method as previously described and was expressed as the number of focus-forming units per milliliter (FFU/mL) [6].

2.9. Western blotting

The purified HCV sample was lysed using a buffer containing 0.1 M Tris–HCl (pH 6.8), 4% SDS, 1.2% 2-mercaptoethanol, 20% glycerol, and Bromophenol blue. SDS–PAGE and immunoblotting were performed as previously described [6]. Antibodies used for immunoblotting were: anti-HCV core (clone 2H9) [6], anti-E1 (B7567) [6], and anti-E2 (clone 8D10-3, unpublished).

2.10. Electron microscopy

Concentrated, purified HCV particles were allowed to settle on carbon-coated copper grids and were stained with 4% uranylacetate. The grids were examined in a transmission electron microscope (H-7650, Hitachi, Tokyo, Japan) and were photographed at an instrumental magnification of 50,000×.

2.11. Sucrose density gradient analysis

The purified HCV sample containing 266 fmol of the HCV core was layered on a stepwise sucrose gradient (10–60%, wt/vol) and was centrifuged for 16 h in an SW41 rotor (Beckman Coulter, Fullerton, CA) at 35,000 rpm at 4 °C. After centrifugation, 12 fractions were harvested from the bottoms of the tubes. For each fraction, the core protein concentration was determined using an immunoassay. The HCV RNA titer was determined using RTD-PCR. The infectious titer was determined using an immunofluorescence assay as described above.

2.12. HCV particle-immunization

The purified HCV particles described above were inactivated by UV-irradiation, and 2 pmol of the HCV core protein of the particles were intraperitoneally injected into 4 week old BALB/c female mice ($n = 3$). Immunization was repeated four times at 2-week intervals (0, 2, 4 and 6 weeks). The Sigma Adjuvant System (Sigma), composed of monophosphoryl lipid A and trehalose dicorynomycolate, was used as an adjuvant. Saline alone was injected into control mice. Sera were collected at 1, 3, 5 and 7 weeks after immunization.

2.13. EIA for measurement of anti-E2 and anti-FLAG antibody responses

Recombinant J6E2/Fc or the FLAG peptide antigen (Sigma) was bound to microtiter plates (Nunc, Rochester, NY, USA) overnight at 4 °C, at a concentration of 50 ng per well. Recombinant J6E2/Fc was produced from COS-1 cells transfected with the CDM-J6E2Fc plasmid, which encodes the J6CF-E2 region (aa 384–720) fused with the Fc region of human IgG. The plates were blocked with Blocking One solution (Nacalai Tesque, Kyoto, Japan) and were washed with PBS containing 0.05% Tween 20 (washing buffer). Serum samples were diluted in washing buffer and were transferred to the blocked, antigen coated plates. After a 1.5-h incubation,

the plates were washed and bound antibody was detected using an HRP-conjugated anti-mouse antibody (GE healthcare, Buckinghamshire, England) and 3,3′,5,5′-tetramethylbenzidine (TMBZ) as a substrate (Sumitomo Bakelite, Tokyo, Japan).

3. Results

3.1. Production of recombinant HCV with an epitope-tagged envelope

To facilitate purification of recombinant HCV particles secreted into the culture medium of transfected cells, we constructed recombinant HCV with a FLAG-epitope-tagged envelope, which could then be purified by affinity chromatography using an anti-FLAG-agarose column. The FLAG-tagged HCV genome J6/JFH-1/3FL with the J6CF structural region was constructed by introducing a triple FLAG-tag sequence into the HVR1 of E2 (Fig. 1A). This region was selected for epitope-tag insertion because we predicted that this region would lie on the outside of the virus particles and would be tolerant to amino acid changes. Recombinant HCV particles were produced following transfection of Huh-7 cells with viral RNA, and were secreted into the culture medium.

RNA-transfected cells were passaged every 4 or 5 days. The level of the HCV core protein in the culture supernatant was measured over a period of 70 days (Fig. 1B). In contrast to the gradually increasing level of the core protein in J6/JFH-1 cells over time, the level of the core protein in the supernatants of the J6/JFH-1/3FL RNA-transfected cells decreased over the first 3 weeks post-transfection. Subsequently, the level began to increase and this level became equal to that of the wild-type J6/JFH-1 RNA-transfected cells 35 days post-transfection. This result suggested that after the first 35 days of culture, some mutations were introduced into the HCV genome that conferred efficient virus production during genome replication and/or that the transfected cells were altered in some way that was more favorable for viral production.

3.2. An N151K mutation facilitates the production of FLAG-tagged HCV

To determine if any adaptive mutations had arisen in the viral genome, we sequenced the full length of the HCV genome on days 8 and 35 post-J6/JFH-1/3FL RNA transfection. On day 8 post-transfection, no non-synonymous mutations were detected. However, on day 35, we found a single amino acid mutation at a potential

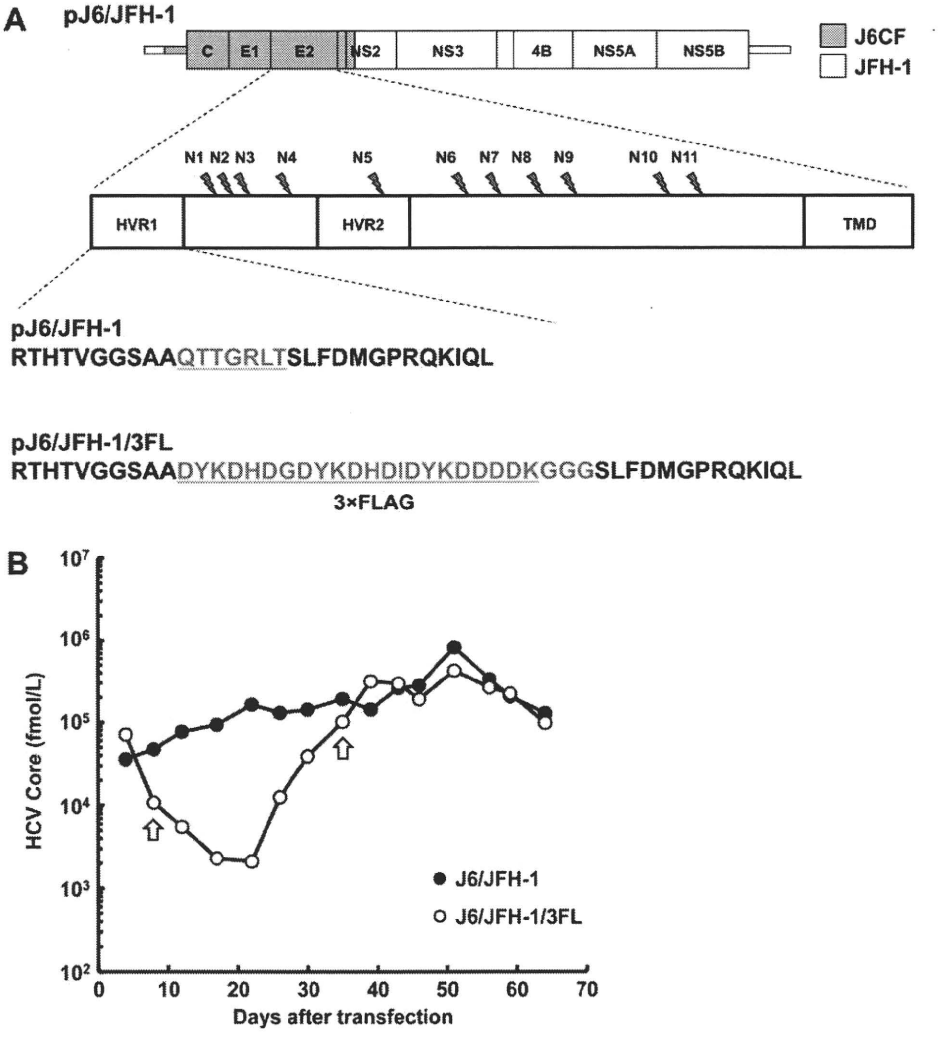

Fig. 1. Time course of HCV core protein secretion in recombinant HCV RNA-transfected cells. (A) Organization of the recombinant HCV construct pJ6/JFH-1/3FL. Open reading frames (thick boxes) are flanked by 5′- and 3′-UTRs (thin boxes). Gray, J6CF; white, JFH-1; HVR, hyper variable region; TMD, transmembrane domain. *N*-Glycosylation sites are indicated by pointers and are numbered N1–N11. The region of pJ6/JFH-1 that is replaced by the 3×FLAG sequence to generate pJ6/JFH-1/3FL is indicated at bottom. (B) HCV core protein secretion into the culture medium after HCV RNA transfection of Huh-7 cells. The HCV core protein was analyzed using an ELISA. Arrows indicate the times at which the J6/JFH-1/3FL HCV genome transfected into HCV RNA-transfected cells was sequenced.

N-glycosylation site of the E2 protein (Fig. 2A) in which asparagine at amino acid position 151 in the E2 protein was changed to lysine (E2N151K). Interestingly, this mutation was identical to that described by Delgrange et al. [12] as a mutation that was important for efficient production of HCV JFH-1. We performed Western blot analysis of cell lysates of transfected cells of different passages, using the anti-FLAG antibody as a probe for E2, to confirm that the N151K mutation abolishes one specific *N*-glycosylation. Indeed, the size of the FLAG-E2 protein was smaller on days 30 and 43 compared to that on day 4 (Fig. 2B). In contrast, the size of FLAG-E2 proteins that were deglycosylated using PNGase F was similar for all of the tested samples (Fig. 2B). This result suggested that the E2N151K mutation abolished *N*-glycosylation at this residue.

To investigate if the E2N151K mutation enhances production of FLAG-tagged HCV, we introduced the E2N151K mutation into the J6/JFH-1/3FL genome (J6/JFH-1/3FL/E2N151K). J6/JFH-1/3FL/E2N151K RNA-transfected cells were then passaged every 4 or 5 days and the level of the HCV core protein in the culture supernatant was measured over a period of 16 days (Fig. 2C). The result clearly showed that the E2N151K mutation contributes to efficient production of FLAG-tagged HCV particles.

We further analyzed the effect of the E2N151K mutation on specific viral infectivity (Table 1). The culture supernatant on day 3 post-transfection of recombinant viral RNA was therefore concentrated by ultrafiltration and tested in an infectious assay. The recombinant virus with the E2N151K mutation exhibited higher specific infectivity than the virus without this mutation. These data suggest that efficient production of infectious particles is impaired by the introduction of a FLAG-tag into the E2 protein but that this deficiency could be compensated for by the introduction of the E2N151K mutation which modifies an *N*-glycosylation site.

3.3. Purification of FLAG-tagged HCV

To purify FLAG-tagged HCV particles, we used a viral construct with a single FLAG-tag, J6/JFH-1/1FL/E2N151K (Fig. 1A), which as efficient in virus production as J6/JFH-1/3FL/E2N151K (data not shown). A total of 10 L of the culture supernatant of Huh-7 cells infected with J6/JFH-1/1FL/E2N151K was collected. This culture medium was concentrated to 300 mL by ultrafiltration and was then subjected to affinity chromatography using an anti-FLAG-agarose column. Bound virus particles were eluted using 10 mL of a

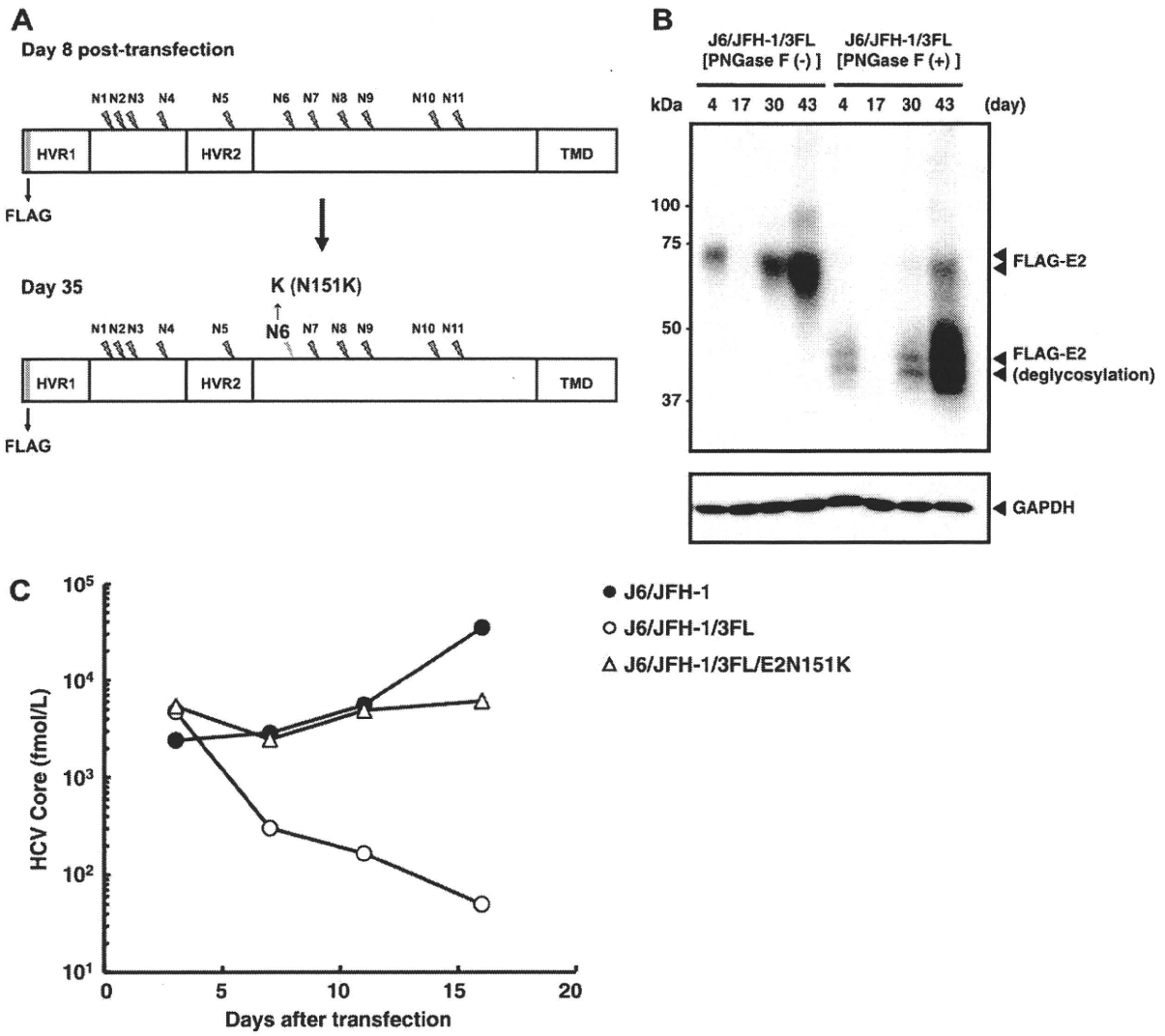

Fig. 2. Characterization of the recombinant HCV genome with an introduced N151K mutation. (A) Schematic diagram of the sequence of the E2 in the J6/JFH-1/3FL HCV RNA-transfected cells on day 8 and day 35 post-transfection. N151K replaces an Asn residue with a Lys residue at the N6 glycosylation site of E2. (B) Western blot analysis of the FLAG-E2 protein in lysates of cells transfected with J6/JFH-1/3FL RNA. Arrowheads indicate intact, and deglycosylated (PNGase F (+)), FLAG-E2 protein (upper panel) and control GAPDH protein (lower panel). (C) HCV core protein secretion into the culture medium following transfection of Huh-7 cells with HCV RNA with or without an introduced N151K mutation.

Table 1
Infectivity of recombinant viruses with or without N151K mutation.

Recombinant virus	Infectious titer ($\times 10^2$ FFU/mL)	HCV core protein ($\times 10^2$ fmol/mL)	Specific infectivity (FFU/HCV core)
J6/JFH-1/3FL	<1.7	1.6	<1.1
J6/JFH-1/3FL/E2N151K	8.3	2.0	4.2

FLAG peptide solution. Finally, the purified HCV particles were concentrated by ultracentrifugation.

The HCV yield and the amount of total protein after each purification step are summarized in Table 2. This purification process resulted in a 5000-fold concentration of the culture supernatant. The recovery of the HCV core protein in the final purified virus preparation was approximately 5%, and the virus purity was increased about 9000-fold compared to its purity in the initial culture medium. Specific infectivity was increased about 4-fold after the final step.

HCV structural proteins in the purified virus sample were examined by Western blotting (Fig. 3A). Core, E1 and E2 proteins were all detected in the purified virus preparation. Interestingly, incorporation of the E2 protein into the purified virus appeared to increase compared to incorporation of the core and E1 proteins. However, this higher apparent incorporation of FLAG-E2, may reflect the presence of free, non-virus incorporated FLAG-E2 proteins that co-purified with the FLAG-tagged virus. We further analyzed the virus particles in the purified preparation by electron microscopy (Fig. 3B–D). Substantial debris was found in the culture

Table 2
HCV yield and properties of purified recombinant HCV after each purification step.

Purification step	Volume (mL)	HCV core protein ($\times 10^2$ fmol/mL)	HCV RNA ($\times 10^7$ copies/mL)	Total protein (μg/mL)	Recovery[a] (%)	Purity[b]	Infectivity ($\times 10^2$ FFU/mL)	Specific infectivity (FFU/HCV core)
Culture supernatant	10,000	1.4	3.5	877	100	1	25	18
Concentrate (after Ultrafiltration)	300	45	57	19,597	96	0.73	743	17
Affinity purification (after Elution)	10	98	324	171	7	469	4240	43
Concentrate (after Ultracentrifugation)	0.2	1440	3220	84	5	9546	94,600	66

[a] Recovery of HCV core protein.
[b] The degree of virus purity was calculated by HCV RNA contents per μg total proteins.

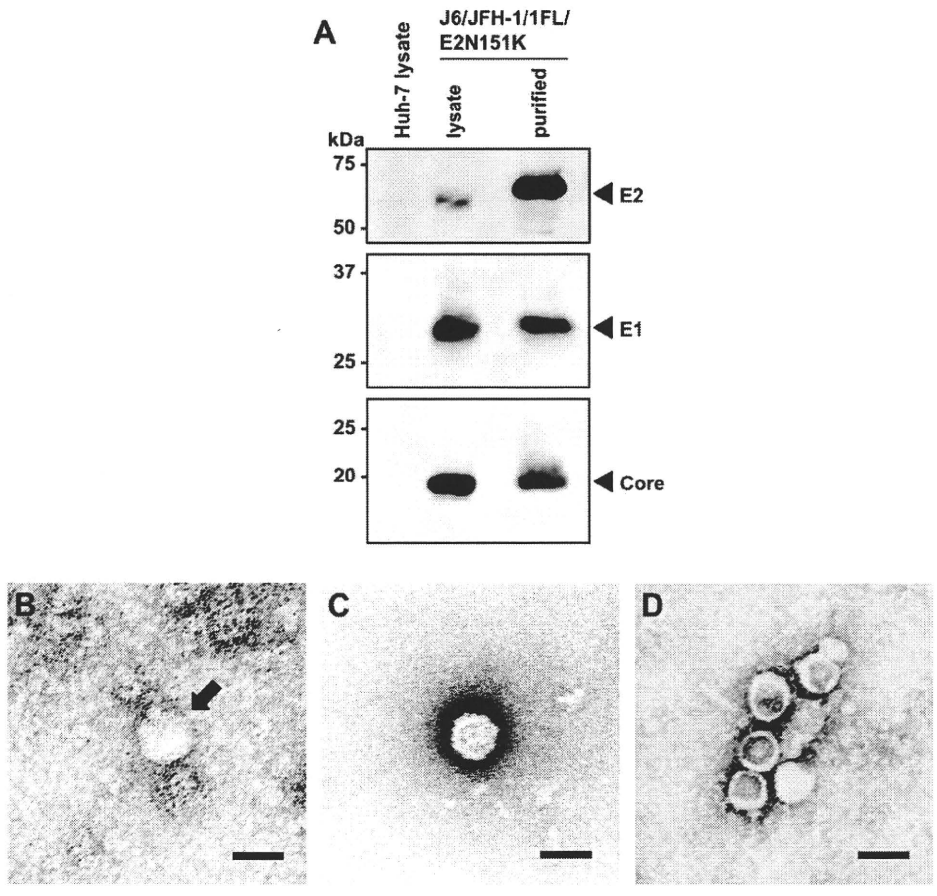

Fig. 3. Analysis of purified HCV particles. (A) Western blot analysis of viral proteins in lysates of, and in HCV particles purified from, whole-cell extracts of Huh-7 cells transfected with J6/JFH-1/1FL N151K RNA. Lysates of non-transfected cells were also analyzed. The arrowheads indicate the positions of the HCV core, E1 and E2 proteins. Marker proteins are shown at left. (B–D) Electron micrographs using negative staining of: (B) An HCV particle from culture media (indicated by an arrow.), (C) A purified HCV particle and (D) Purified HCV particles aggregated by an anti-FLAG antibody. Scale bar, 50 nm.

supernatant concentrated by ultrafiltration, which made it difficult to identify virus particles (Fig. 3B). In contrast, spherical particle structures of 40–60 nm could be clearly observed in the purified samples (Fig. 3C and D). Furthermore, the purified FLAG-tagged HCV particles were aggregated by the anti-FLAG antibody (Fig. 3D). The size and morphology of the FLAG-tagged particles were similar to each other but with slight deviations. The combined data suggest that the FLAG-tagged HCV particles can be purified by affinity chromatography using anti-FLAG-agarose.

3.4. Physical properties of purified FLAG-tagged HCV

We next further analyzed the properties of the purified FLAG-tagged HCV particles. The total number of proteins in the purified viral sample, as judged by SDS–PAGE and silver staining analysis, was much lower than that in the original culture medium (Fig. 4A). We confirmed by mass spectrometry analysis that these extra protein bands in the purified preparation were not viral proteins but were host proteins that bound to the FLAG-agarose (data not shown).

We further analyzed the purified FLAG-tagged HCV particles using a sucrose density gradient (Fig 4B). Purified virus was layered on top of a preformed continuous 10–60% sucrose gradient and was then centrifuged. Twelve fractions were collected and the HCV core protein, RNA and viral infectivity were determined for each fraction. The HCV particles migrated at a density between 1.13 and 1.16 g sucrose/mL. The density at which the peak of the HCV core protein was observed was almost identical to the density at which the HCV RNA and infectivity were detected.

3.5. Immunogenicity of purified HCV particles

To examine the immunogenicity of the FLAG-tagged HCV particles, they were injected into BALB/c mice and the sera of these mice were then analyzed for reactivity with recombinant J6E2/Fc or the FLAG peptide using an ELISA. The HCV particles were inactivated by UV-irradiation prior to injection using the Sigma Adjuvant System as an adjuvant. Both anti-E2 and anti-FLAG antibodies were induced in mice sera after four immunizations (Fig. 4C). These results suggested that the envelope proteins of the FLAG-tagged HCV

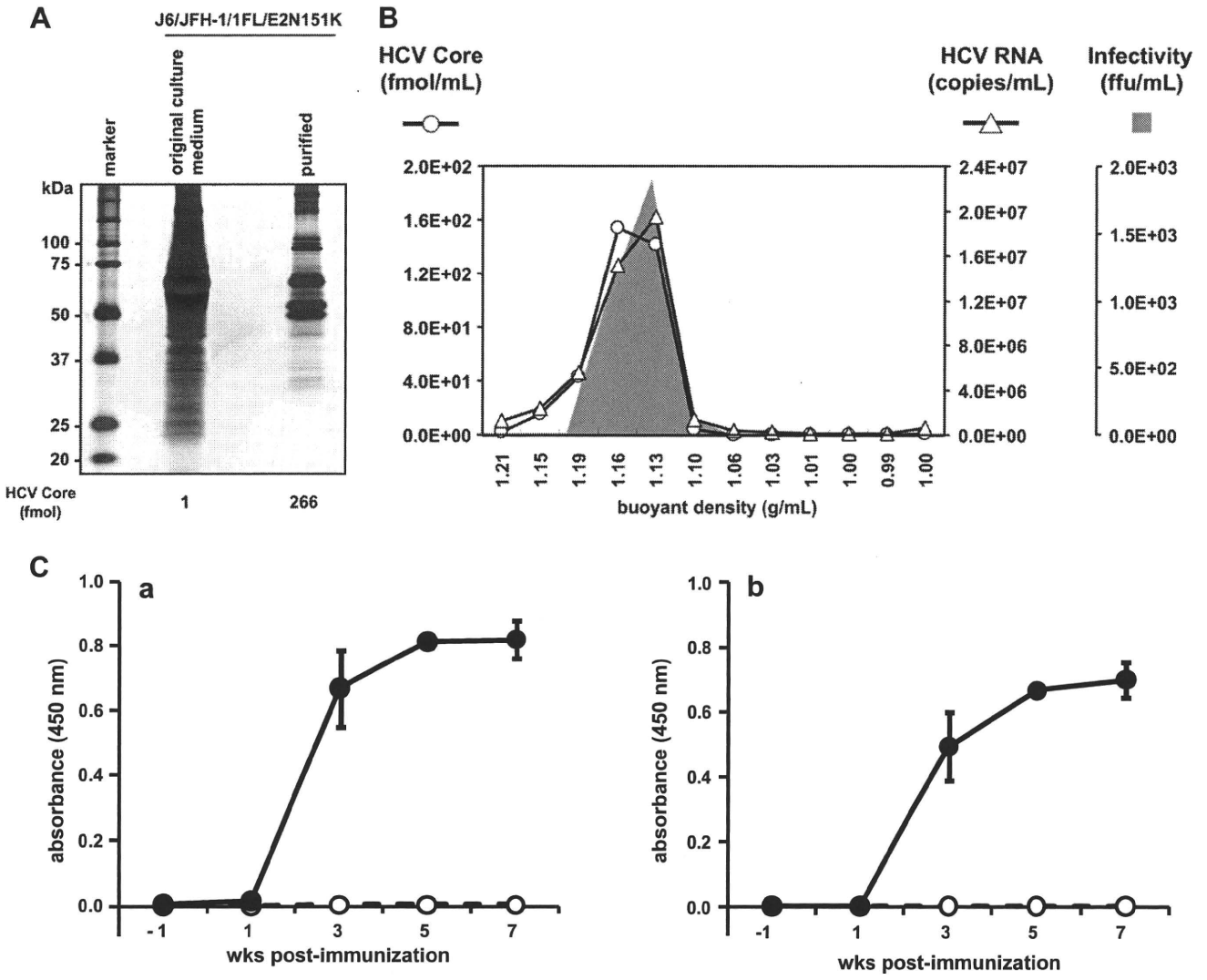

Fig. 4. Physical properties and immunogenicity of purified HCV particles. (A) Silver staining of non-purified (original culture medium) and purified HCV samples. The non-purified and purified samples contained 1 and 266 fmol, respectively, of the HCV core. (B) Sucrose density gradient analysis of purified HCV particles. The level of the HCV core protein (open circles), HCV RNA (open triangles) and the HCV infectivity towards naïve Huh-7 cells (shown in gray) were analyzed for each fraction as described in Section 2. (C) Purified HCV particles (closed circles) or saline (open circles) were intraperitoneally injected into BALB/c mice ($n = 3$), and sera were collected at the indicated times. The collected sera were examined for the presence of anti-E2 (a) and anti-FLAG (b) antibodies using the J6E2/Fc protein and the FLAG peptide as antigens in an EIA as described in Section 2.